International
Progress Report

IPR-07-01

Äspö Hard Rock Laboratory

Prototype Repository

Thermal 3D modelling of Äspö Prototype Repository

Ola Kristensson
Harald Hökmark

Clay Technology AB

May 2007

Svensk Kärnbränslehantering AB
Swedish Nuclear Fuel
and Waste Management Co
Box 5864
SE-102 40 Stockholm Sweden
Tel 08-459 84 00
+46 8 459 84 00
Fax 08-661 57 19
+46 8 661 57 19

Äspö Hard Rock Laboratory

Report no.
IPR-07-01
No.
F63K
Author
Ola Kristensson
Harald Hökmark
Date
May 2007
Checked by
Niclas Bockgård
Date
September 2007
Approved
Anders Sjöland
Date
2007-09-07

Äspö Hard Rock Laboratory

Prototype Repository

Thermal 3D modelling of Äspö Prototype Repository

Ola Kristensson
Harald Hökmark

Clay Technology AB

May 2007

Keywords: Prototype Repository, 3D thermal modelling, Rock thermal conductivity, Code_Bright, Rock wall temperature, Canister surface heat flux

Abstract

This report deals with 3D modeling of the temperature evolution in the Prototype Repository.

The simulated canister heat flux and the rock wall temperature at canister mid-height are found to be appropriate as thermal boundary conditions for models on a smaller scale.

The rock mass temperature at canister mid-height can be reproduced with satisfactory accuracy using one global thermal rock conductivity.

A model, incorporating higher tunnel floor thermal conductivity and decreasing background temperature, is used for calibrating the thermal conductivity in the rest of the rock mass by minimizing the difference between measured and simulated temperatures in the rock pillars. This model appears to reproduce the measured temperatures at all important points within about 1 °C.

Finally, the influence of changing the backfill conductivity and incorporating tunnel convection are found not to have any significant effect on the temperatures at canister mid-height.

Sammanfattning

Rapporten behandlar termiska processer i Prototypförvaret. En termisk kontinummodell som representerar förvaret i tre dimensioner har utvecklats för och lösts med hjälp av finita elementprogrammet Code_Bright. Tyngdpunkten i arbetet ligger på jämförelser mellan uppmätta och simulerade temperaturer i berget. För att få en noggrann modell följer de individuella kapslarnas värmelaster noggrant de i experimentet uppmätta.

De två huvudsakliga målen med arbetet är att:

- Ta fram termiska randvillkor till modeller på en mindre skala.
- Undersöka hur väl en modell med ett enda, globalt värde på bergets termiska konduktivitet reproducerar uppmätta bergtemperaturer nära de sex kapslarna.

Kapslarnas värmeflöde per enhet kapselyta och bergväggstemperaturerna på kapslarnas höjdcentrum har funnits lämpliga för användning som termiska randvillkor för modeller på en mindre skala.

Bergmassans temperatur vid samma höjd som kapselns höjdcentrum kan återskapas med tillfredställande noggrannhet med användande av ett enda globalt värde på bergets termiska konduktivitet.

Numeriska simuleringar som föregått den här studien har visat att tunnelgolvet i modellen kan behöva tilldelas en högre termisk konduktivitet jämfört med resten av bergmassan.. Berguttaget och ventilationen före och under installation av försöket har förmodligen gett en störning av bakgrundstemperaturen vid experimentplatsen och som en konsekvens av detta minskar den effektiva bakgrundstemperaturen. Minskningen kan vara cirka 0,2 °C/år /Sundberg et al. 2005/. En modell har utvecklats där den termiska konduktiviteten i berget är kalibrerad mot uppmätta bergtemperaturer för fallet med ändrad konduktivitet i tunnelgolvet och evolution av bakgrundstemperaturen. Överensstämmelsen mellan bergstemperaturen i experiment och simuleringar förbättras ytterligare med denna modell där det framkalibrerade värdet på bergkonduktiviteten används. Den här modellen verkar återskapa de uppmätta temperaturerna i de viktigaste mätpunkterna (det vill säga nära kapslarna) inom ett fel på 1 °C.

Det är modellen med det framkalibrerade värdet på bergkonduktiviteten som anses representera de i verkligheten förekommande termiska processerna i bergmassan bäst i denna rapport.

Slutligen har influensen av förändringar i återfyllnadens termiska konduktivitet och införlivandet av tunnelkonvektion konstaterats vara insignifikant med avseende på temperaturen på höjdcentrum av kapslarna.

Executive summary

This report treats thermal processes in the Prototype Repository. A thermal continuum model with a three dimensional representation of the experimental geometry is developed for and solved using the finite element program Code_Bright. The focus is on comparisons between experimentally found and simulated temperatures in the rock mass. In order to obtain an accurate model the individual canister heat loads in the model follow the experimentally monitored heat loads closely.

The two main objectives are:

- Obtain thermal boundary conditions for models on a smaller scale.
- Investigate how well a model using one discrete global value of the thermal rock conductivity reproduces rock temperatures measured close to the six canisters.

The simulated canister surface heat flux and the rock wall temperature at canister mid-height are found to be appropriate as thermal boundary conditions for models on a smaller scale.

The rock mass temperature at canister mid-height can be reproduced with satisfactory accuracy using one global thermal rock conductivity.

In numerical simulations preceding this study, it has been found that the tunnel floor in the model may have to be allotted higher thermal conductivity as compared to the rest of the rock mass. The excavation process and the ventilation before and during the installation of the experiment may have given a disturbance of the background temperature at the experimental site, and as a consequence the effective background temperature decreases. That decrease may amount to about 0.2 °C/year /Sundberg et al. 2005/. A model is developed where the thermal conductivity in the rock is calibrated by comparing the difference in rock temperatures for the case where the changed tunnel floor property and the background temperature evolution are considered. The similarity between the rock temperatures in the experiment and the model were improved using the model with the calibrated thermal conductivity value. This model appears to reproduce the measured temperatures at the most important points (i.e. those close to the canisters) within about 1 °C.

It is the model using the calibrated value of the rock conductivity that is considered to represent the thermal processes in the real experiment most accurate in this report.

Finally, the influence of changing the backfill thermal conductivity and incorporating tunnel convection are found not to have any significant effect on the temperatures at canister mid-height.

Contents

1 Introduction

The Prototype Repository Project simulates a part of a KBS-3 nuclear waste repository /Börgesson et al., 2002/. Within the Prototype Repository project the performance of such a repository on the 50 m scale during the first years after deposition can be tested. The behavior of the system is monitored by use of numerous instruments of different types positioned in the nearfield rock, in the electrically heated canisters and in the bentonite buffer. The Prototype Repository also offers a great possibility to investigate to what extent models agree with reality.

Figure 1-1 shows the geometry of the experiment and in Table 1-1 some geometrical data is shown. The Prototype Repository consists of two sections. The first, inner, section contains four full-scale deposition holes, each with a canister and a surrounding bentonite buffer, and the second, outer, section contains two such holes. The tunnel and the 1 m top parts of the deposition holes are filled with backfill material, consisting of bentonite and crushed rock. The sections are separated by a concrete plug to allow for separate dismantling and different test times. There is an additional outer plug to confine the experiment mechanically and hydraulically and to simulate the conditions in a real repository. To simulate the thermal behavior of the nuclear waste, heaters are installed in the canisters.

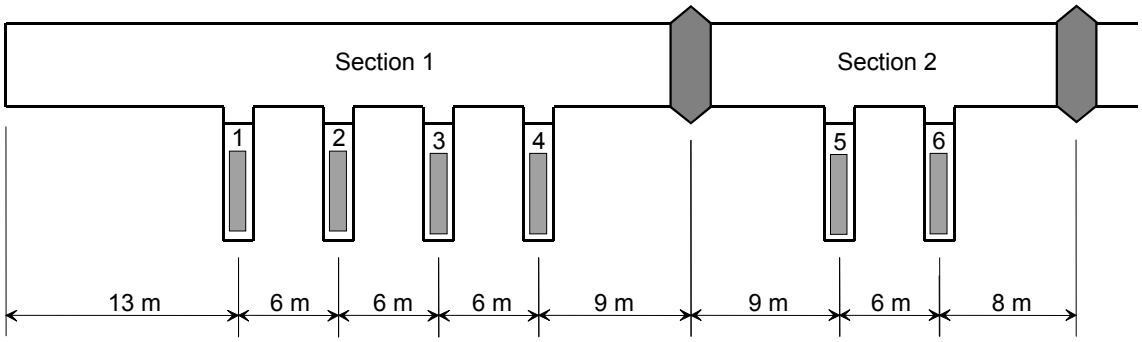

Figure 1-1 *Geometry of the Prototype Repository.*

Table 1-1. Geometric data of the Prototype Repository.

Deposition hole depth	8 m	Bentonite thickness above the canister	1,5 m
Deposition hole diameter	1,75 m	Total tunnel length	63 m
Canister height	~5 m	Length of section I	40 m
Canister diameter	1,05 m	Length of section II	23 m
Bentonite thickness below the canister	0,5 m	Tunnel diameter	5 m

2 Objectives

Here, a three-dimensional continuum model is developed to simulate the thermal behavior of the Prototype Repository Project. The focus is on the temperature in the rock, and in particular on comparisons between calculated rock temperatures and temperatures measured at a number of points in the rock mass. A finite element program, Code_Bright, is used to solve the problem numerically.

The 3D thermal analysis has two main objectives:

- Find relevant time-dependent thermal boundary conditions for local THM models of the individual deposition holes. These models will be used to analyze the behavior of the buffer material during heating and water uptake.
- Investigate how well the measured rock temperatures can be reproduced assuming one global and constant value of the rock heat conductivity. Measurements on laboratory-scale samples from the Prototype Repository rock mass indicate that there is a conductivity variation.

In addition there are the following objectives:

- Check the influence of the backfill thermal properties on the overall thermal development around canister mid-height, i.e. the region where maximum canister temperatures are expected, and in the canister top region, i.e. where the bentonite temperature will be at maximum in dry deposition holes (Note: in dry deposition holes with unsaturated bentonite there will be direct canister-buffer contact at the top and bottom surfaces, but probably not at the mid-section).
- Explore the effect of the open ventilated tunnel outside the plug confining the experiment. This is made here to ensure that the way the open tunnel is represented does not cause any irrelevant influence on the calculated Prototype Repository rock mass temperatures.

3 Model description

A three-dimensional thermal continuum model of the prototype repository has been developed using Code_Bright, a finite element code developed at the University of Barcelona /CIMNE, 2002/. Code_Bright has been developed specifically to analyze coupled THM processes in porous saturated and unsaturated geological media.

3.1 Geometry

The three-dimensional model contains the experimental geometry, where tunnel, plugs, backfill, buffer, and canisters are present, see Figure 3-1. The experimental geometry is embedded in a large rock mass denoted embedment in the forthcoming.

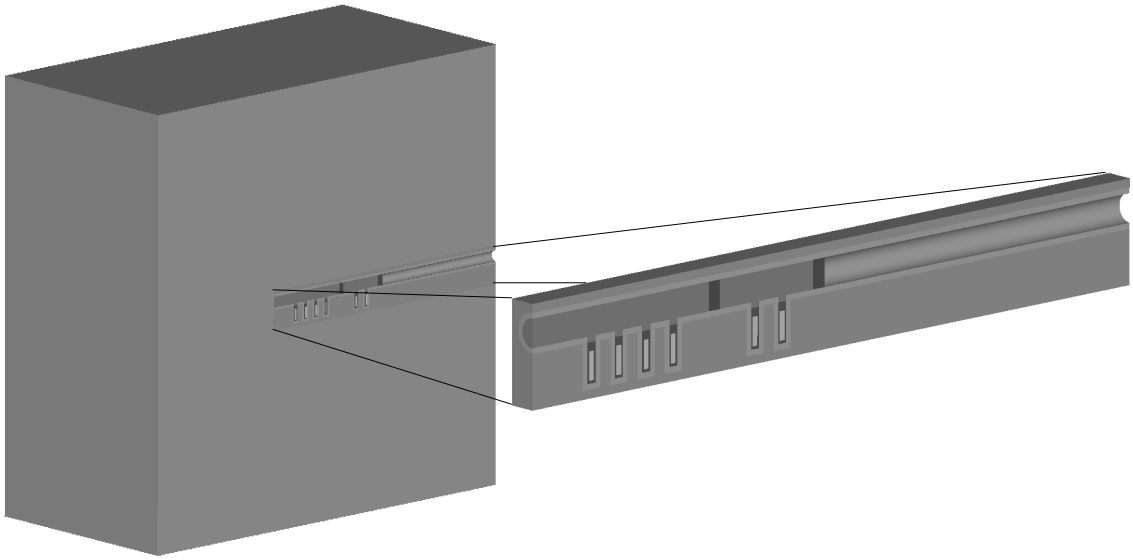

Figure 3-1. *Model geometry. The experimental geometry section (shown in the up-scaled figure) is surrounded by a large embedment.*

As seen in Figure 3-1 an assumption of a vertical symmetry plane through the tunnel has been adopted. The symmetry assumption was made in order to reduce the size of the problem. The outer dimensions of the problem domain are 200×200×200 m (*length*×*width*×*height*), which considering the symmetry becomes 200×100×200 m.

The finite element model of the base case, defined below, contains 86119 tetrahedral elements with linear shape functions. There are 17628 nodes in the model, and since the model is purely thermal, the degrees of freedom equal the number of nodes. The element density is greatest at the canister positions, and decreases with increasing distance from the canisters. The shortest element sides are approximately 0.2 m and at the embedment surface the element sides are approximately 30 m.

3.2 Material properties

All heat transport is assumed to take place by linear heat conduction in homogenous isotropic media. A number of cases are considered, and one special base case has been adopted which serves as reference from which changes are made.

3.2.1 Base Case

The parameters used in the base case model are found in Table 3-1, where ρ is the solid phase density, λ denotes the thermal conductivity and c is the specific heat.

Table 3-1. Material parameter values used in the base case model.

Material	ρ [kg/ m^3]	λ [W/(m·K)]	c [J/(kg·K)]
Rock/plug	2770	2.72	770
Backfill	2500	1.5	780
Bentonite	2780	1.0	800
Canister	8930	390	390

The material properties for the rock are close to the ones used in the numerical model adopted in /Sundberg et al., 2005/, where the Prototype Repository rock mass thermal conductivity of 2.72 W/(m·K) was obtained by inverse modeling between day 160 and day 525. The volumetric heat capacity of the rock was 2.2 MJ/(m^3·K) in /Sundberg et al., 2005/ and is 2.1 MJ/(m^3·K) in this report.

The backfill properties are close to the properties used in /Börgesson and Hernelind, 1999/ except for a lower value of the specific heat, 780 J/(kg·K) as compared to 1000 J/(kg·K).

The bentonite properties are also taken from /Börgesson and Hernelind, 1999/. The bentonite conductivity (1.0 W/(m·K)) is the reference value used in SKB's canister spacing guidelines /SKB, 2004/.

The canister parameters are tabulated handbook copper values. The 5 cm conductive copper shell redistributes the heat generated by the electrical heaters in the interior of the canisters, meaning that, for the purpose of this study, the material properties and the geometrical details of the canister interior do not need to be explicitly represented.

3.2.2 Additional cases

In addition to the base case several other cases have been considered where different properties were changed in order to study the impact on the thermal response. Table 3-2 shows an overview of the different cases, where the parameter settings are indicated for the individual cases.

To investigate the influence on the temperature evolution of the rock conductivity, four different values were tried. Values used here are 2.72, 2.65, 2.52, and 2.685 W/(m·K). The first two values are reported in /Sundberg et al 2005/ as results of inverse modeling of the Prototype Repository experiment using recordings from a large number of

thermocouples installed at different positions in the Prototype Repository rock mass. The third value is a prognosis based on the mean value of results from laboratory-scale tests on samples from the Prototype Repository rock mass /Sundberg et al., 2005/. The value 2.685 W/(m·K) is obtained using a simple optimization scheme with respect to the simulated temperature deviation from the experimental ones.

In /Sundberg et al 2005/ it was found, by using inverse modeling, that the temperatures measured in the rock situated close to the tunnel floor indicated that there is a higher rock thermal conductivity in the tunnel floor region as compared to the conductivity in the main part of the rock mass. Therefore models were analyzed assuming the floor region to have a higher conductivity of 3.5 W/(m·K). This value was obtained from /Sundberg et al 2005/.

In /Sundberg et al 2005/ it was also argued that a decreasing background temperature, 0.2 °C/year, could affect the apparent temperature response. During the excavation the background temperature increased due to heat produced by machinery etc. In order to investigate this, the results from the actual simulations were post-processed, i.e. a linear decrease in temperature was subtracted from the obtained temperature data.

Finally the influence of backfill conductivity and convective tunnel conditions on temperature were investigated. In the backfill conductivity study the values 1.0 or 2.72 W/(m·K) were used, which corresponds to the values of the bentonite and rock respectively. Table 3-2 shows an overview of the models analyzed here.

Table 3-2. Case overview.

Case Nr	*Rock conductivity (rest) (W/(m·K))*	*Rock conductivity (floor region) (W/(m·K))*	*Background temperature (°C)*	*Backfill Conductivity (W/(m·K))*	*Tunnel condition*
Case 1 (base case)	2.72	2.72	15	1.5	adiabatic
Case 2	2.72	2.72	15-0.2/year	1.5	adiabatic
Case 3	2.72	3.5	15	1.5	adiabatic
Case 4	2.72	3.5	15-0.2/year	1.5	adiabatic
Case 5	2.65	2.65	15	1.5	adiabatic
Case 6	2.65	2.65	15-0.2/year	1.5	adiabatic
Case 7	2.65	3.5	15	1.5	adiabatic
Case 8	2.65	3.5	15-0.2/year	1.5	adiabatic
Case 9	2.52	2.52	15	1.5	adiabatic
Case 10	2.52	2.52	15-0.2/year	1.5	adiabatic
Case 11	2.52	3.5	15	1.5	adiabatic
Case 12	2.52	3.5	15-0.2/year	1.5	adiabatic
Case 13	2.685	3.5	15-0.2/year	1.5	adiabatic
Case 14	2.72	2.72	15	1.0	adiabatic
Case 15	2.72	2.72	15	2.72	adiabatic
Case 16	2.72	2.72	15	1.5	convective

In addition to the cases shown in Table 3-2, simulations where the mesh dependency was studied have also been conducted.

3.3 Boundary conditions, initial conditions and thermal load

Adiabatic conditions are adopted at all boundary surfaces in the base case model and the initial temperature is set to 15 °C in the entire model.

The thermal load was prescribed as canister power. The best way to give the correct load in the Code_Bright model was to prescribe the power per node along the center lines of the individual canister cylinders.

The input power to was obtained by fitting a piecewise linear function to the canister power recorded in the experiment /Goudarzi and Johannesson, 2006/. In this way the most prominent features of the thermal load are accounted for in the model. In the compilation of graphs in Figure 3-2 and Figure 3-3, the functions approximating the canister power are shown along with the recorded values.

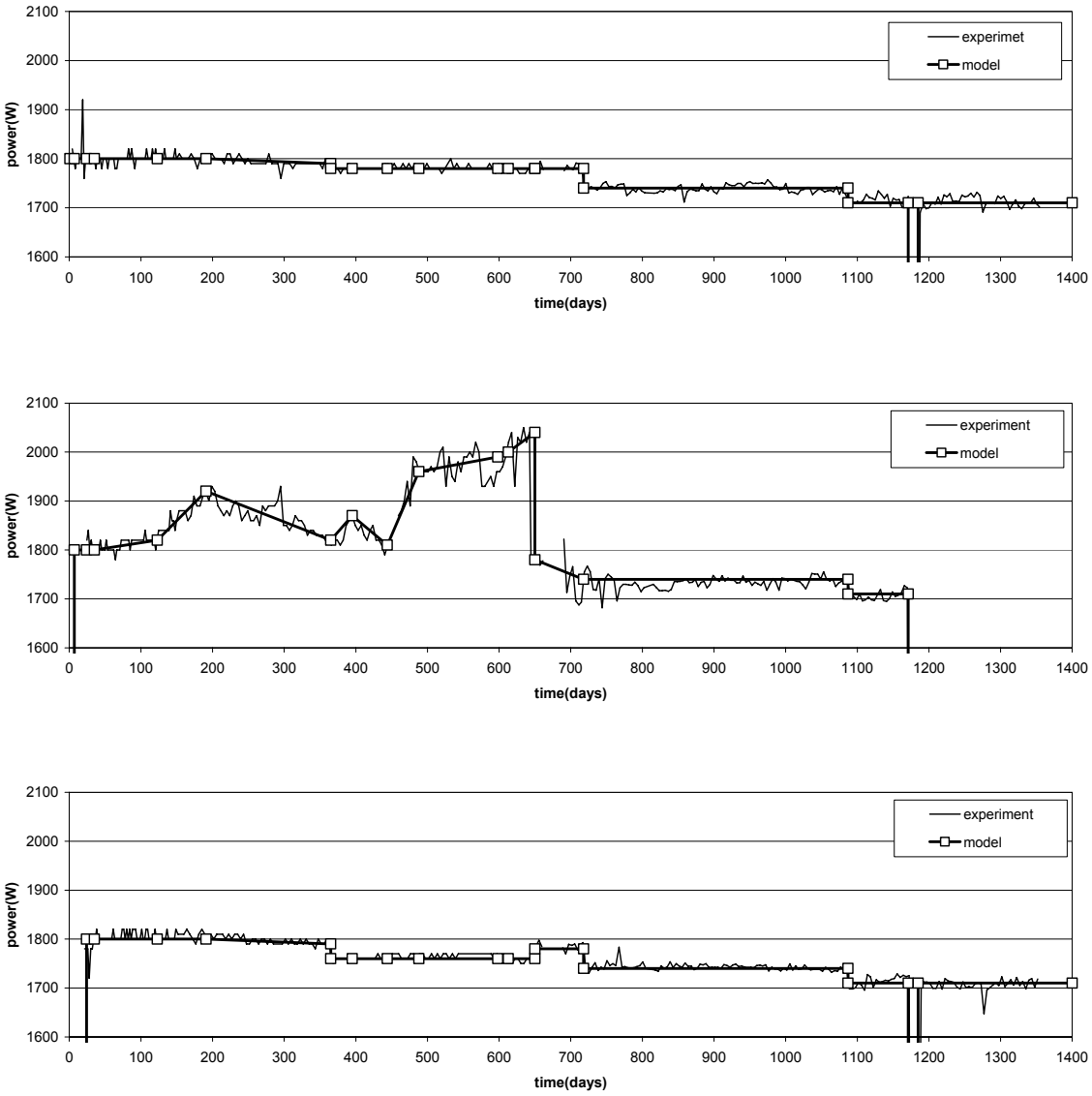

Figure 3-2. *Power of canister 1(top), 2 (center) and 3 (bottom).*

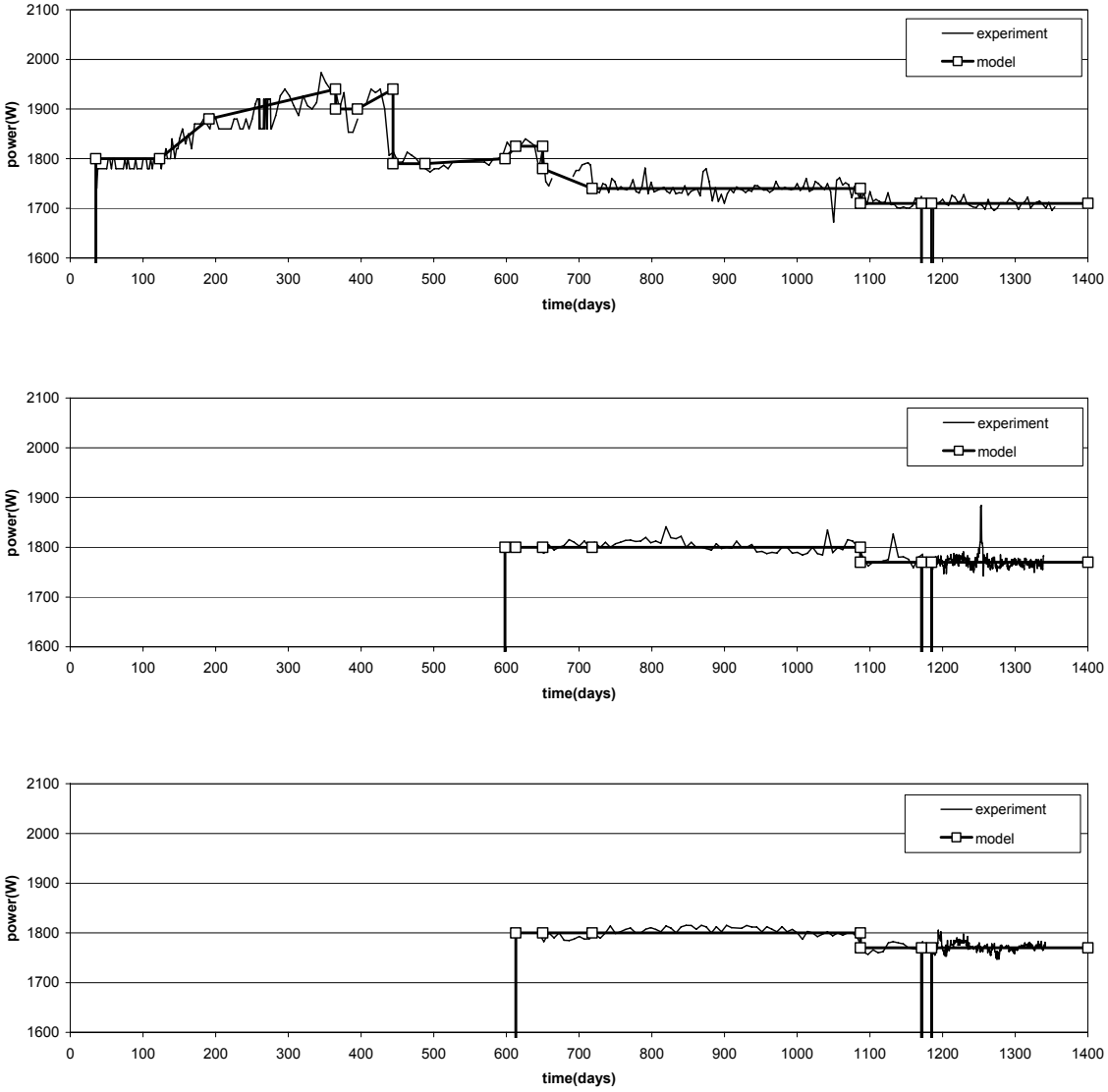

Figure 3-3. *Power of canister 4 (top), 5 (center) and 6 (bottom).*

4 Results

In this section the results from the models are shown and commented. When nothing else is noted, the results concern the base case. First, the mesh dependence is investigated. Then the heat flux at the canister surface is studied. After this, the rock temperatures are compared with the recorded temperatures in some closely situated points. Finally, the base case model is compared to models with changed thermal conductivity of the backfill and with tunnel convection conditions.

4.1 Mesh dependence

Here the temperature and the heat flux response dependency on the mesh density around the first canister are studied. The mesh is refined from the base case mesh density at the canister surface and the canister center line. Initially, in the base case, the element side length is approx. 0.2 m in the canister region. Two successive refinements with the element side length set to 0.15 m and 0.12 m at the canister surface respectively and the element side length 0.15 m at the canister center line are used in the mesh dependency study.

The temperature at the surface of the canister along a vertical cut in the tunnel direction is shown in Figure 4-1 for the different mesh alternatives at day 1400. The result shows that the temperature increases when the mesh is refined. This probably comes from the capacity of the fine mesh to resolve the temperature field to a higher degree and represent the temperature gradient more correctly. The temperature difference between the 0.2 and 0.12 mesh side length is less then one degree Celsius or approximately one percent of the magnitude. Thus, the temperature around the canister shows no sign of being critically mesh dependent using the mesh density adopted in the model.

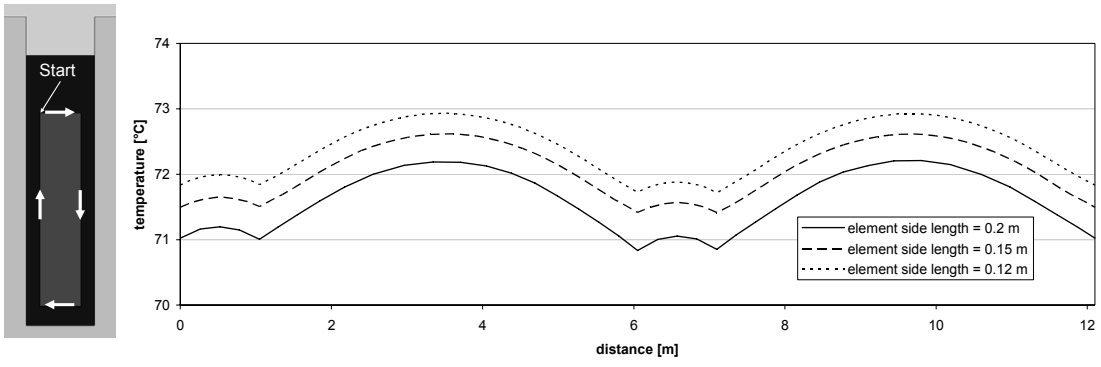

Figure 4-1. *Canister surface temperature for three mesh alternatives, canister 1.*

In Figure 4-2 the horizontal heat flux at the canister surface along the same vertical cut through the canister as for the temperature but now as a function of the depth is shown. Also here the situation regards day 1400. The horizontal flux is taken as positive in the direction of the tunnel opening. A "dog bone"-shaped profile of horizontal heat flux is obtained. The characteristic flux profile comes from:

- More canister surface per unit of canister height in the end sections.
- More efficient cooling of the surface in the edge regions.

The flux response along the canister is not as smooth as the temperature response. This comes from the characteristics of the used discretization scheme together with the way the flux results are represented. In this analysis tetrahedral elements with linear shape functions are used which gives rise to one integration point in each element. Thus, the flux is represented with a constant vector in each element. The result shown in Figure 4-2 is obtained by interpolating the constant vectors from the elements to the associated nodes using some interpolation scheme and will therefore be dependent on the actual mesh geometry in the surrounding area. However, there is no obvious, systematic mesh dependence.

To confirm whether the magnitude of the simulated canister mid-height heat flux is reasonable it is compared with a value obtained using an analytical expression suggested in /Hökmark and Fälth, 2003/. The analytical expression of the mid-height heat flux $q_r(r_0)$, is given in terms of the total canister power Q, the canister area $A = 2\pi r_0(h + r_0)$, where $r_0 = 0.525$ m is the canister radius and $h = 5$ m is the canister height. The 0.92 reduction factor accounts for the non-uniform heat output, i.e. with more surface flux around the edges and less around mid-height.

$$q_r(r_0) = 0.92Q / A \tag{1}$$

At day 1400, when the canister power Q is 1710 W, the mid-height heat flux is 86.3 W/m^2 according to the analytical expression. The analytical mid-height value is indicated with a thick line for both a positive and a negative sign in Figure 4-2. At the mid-height of the canister, around the 5 m depth mark, the numerically simulated heat flux corresponds well with that of the analytically obtained value. The mesh with the finest density around the canister produces a flux very close to the analytical value.

The calculated results regard canister 1, meaning that there is a small asymmetry caused by the heat output from the neighbor canister on the right hand side. That effect can be seen with some difficulty in the profile plot (i.e. the fine mesh profile indicates flux values a little larger than 86.3 W/m^2 on the left hand side and a little less on the right hand side. This is demonstrated in some more detail in following sections.

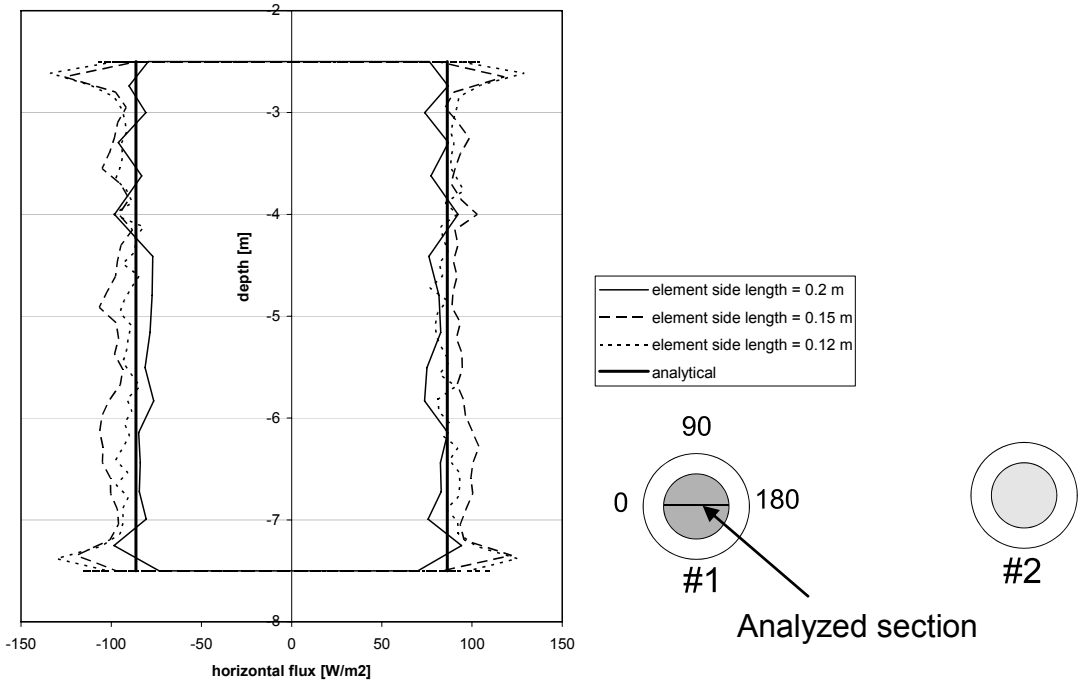

Figure 4-2. *Horizontal surface heat flux of canister 1 after 1400 days for three mesh alternatives. The analytical value is valid only at mid-height. The vertical section is along the tunnel. Neighbor canisters are to the right in the picture.*

4.2 Heat flux investigation

The correctness and character of the heat flux is discussed in detail below for canister 1 and canister 3. The magnitude of the heat flux is checked against the analytical expression. The asymmetry of the heat flux field is investigated. Also, the heat flux is checked by back-calculating the bentonite conductivity from it and evaluate whether the obtained value is reasonable. When considering the heat flux, the mesh alternative with the finest mesh density has been used in order to obtain detailed representations.

4.2.1 Canister 1

At day 395 in the experiment, the power of canister 1 is Q = 1780 W according to the experimental data. 395 days from the startup is chosen as a suitable time for these investigations since transients should be vanished at this instant. When using Equation 1 we obtain $q_r(r_0)$ = 89.85 W/m^2.

Figure 4-3 shows the horizontal surface heat flux after 395 days obtained from the model. The vertical section is along the tunnel. Neighbor canisters are to the right (positive flux at θ = 180 °, i.e. in the direction of the tunnel opening). The horizontal flux is shown as a function of depth below the tunnel floor.

Figure 4-4 shows the mid-height surface flux surface in three different directions: 0º (tunnel face), 90º (normal to tunnel) and 180º (tunnel opening). These curves are obtained as the average at depths between 4 m and 6 m below the tunnel floor (Note that Figure 4-3 verifies that the average flux in this height section would be a good approximation of the mid-height flux). At day 395 the model gives $q_r(0,r_0)$ = 94.73

W/m^2 and $q_r(180,r_0)$ = 81.93 W/m^2 for canister 1. The mean value of the radial heat flux in the two directions is q_{mean} = 88.3 W/m^2 which is 1.7 % less than the analytical value. In the model $q_r(90,r_0)$ = 91.36 W/m^2 which is 1.7 % higher than the analytical value. This indicates that the heat flux obtained in the numerical model agrees well with the analytically obtained value.

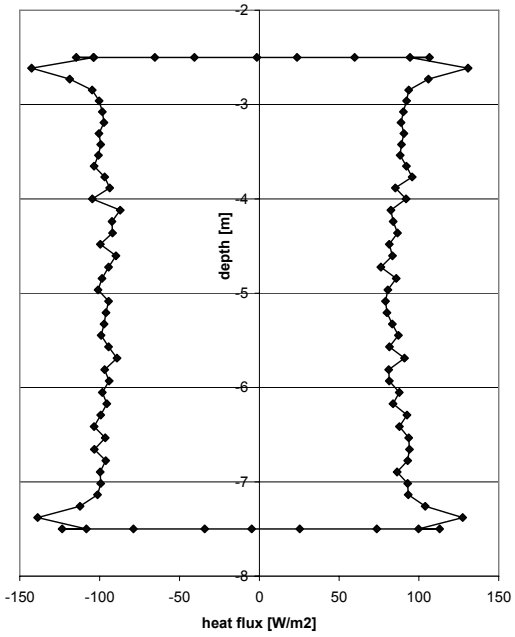

Figure 4-3. *Horizontal heat flux around canister 1. In the height section between 4 and 6 m, there are no systematic variations, meaning that the section average is valid approximation of the mid-height flux.*

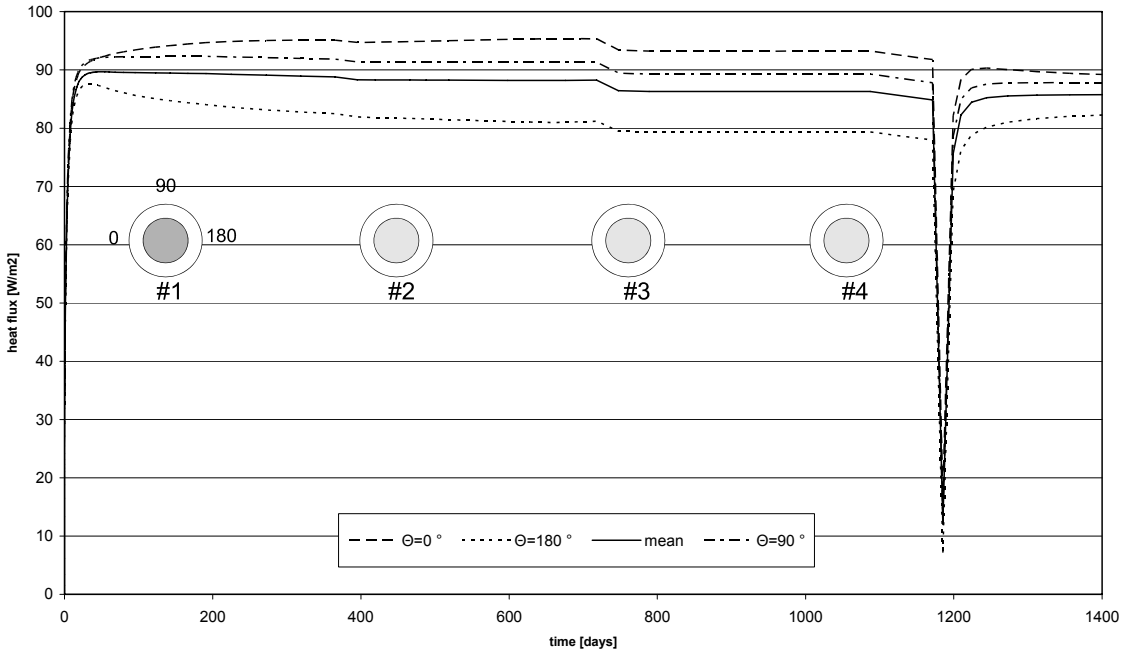

Figure 4-4. *Canister 1 heat fluxes. The canister surface heat flux history is shown for θ = 0, 90, 180 ° and the mean value of θ = 0 and 180 °.*

4.2.2 Canister 3

At day 395 in the experiment, the power of canister 3 is Q = 1760 W according to the experimental data. When using Equation 1 we obtain $q_r(r_0)$ = 88.84 W/m^2.

The horizontal heat flux profile for canister 3 at day 395 obtained in the 3D model is shown in Figure 4-5.

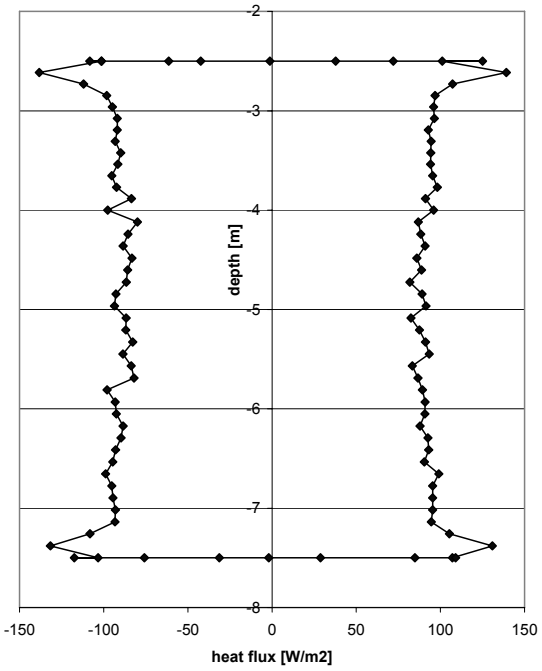

Figure 4-5. *Horizontal heat flux around canister 3.*

The average heat flux at depths between -4 m and -6 m at day 395 is $q_r(0,r_0)$ = 87.35 W/m^2 and $q_r(180,r_0)$ = 88.02 W/m^2 for canister 3. The mean value of the radial heat flux in the two directions is q_{mean} = 87.67 W/m^2 which is 1.3 % off the analytical value. The obtained perpendicular heat flux is $q_r(90,r_0)$ = 91.06 W/m^2 which differs with 2.5 % from the analytical value.

The canister surface heat flux history is shown for θ = 0, 90, 180 ° and the mean value of θ = 0, 180 ° in Figure 4-6.

When comparing the flux history plot between canister 1 and canister 3 it can be seen that at canister 1 there is more asymmetry as compared to canister 3. Since canister 1 only has neighboring canisters at one side the flux field has an asymmetric contribution from the other canisters. Canister 3 has neighboring canisters on both sides and will therefore have a less asymmetric flux field.

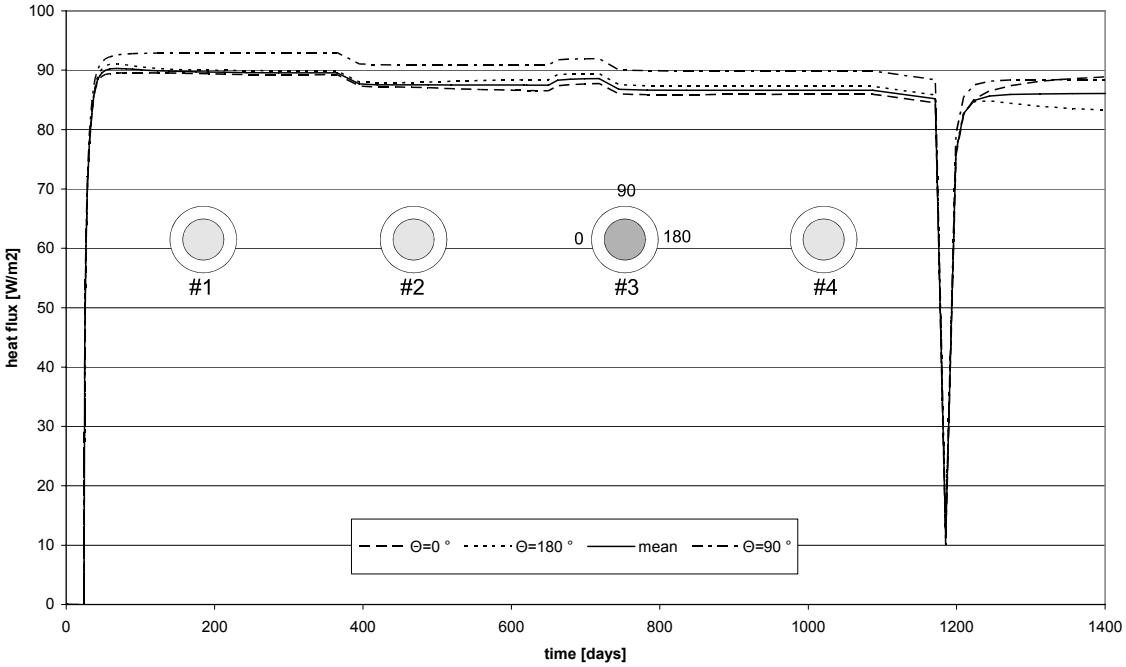

Figure 4-6. *Canister 3 heat fluxes.*

4.3 Bentonite conductivity check

To further investigate the calculated flux at the canister surface, the bentonite conductivity is calculated between two temperature sensor locations using the position of the sensors, the sensor temperatures and the calculated flux in an analytical expression. The obtained magnitudes of the bentonite conductivity are then used as indicators whether the input fluxes are reasonable.

The analytical expression contains the calculated radial canister surface heat flux $q_r(\theta,r_0)$, where r_0 = 0.525 m, and measured temperatures $T(\theta,r_1)$ and $T(\theta,r_2)$ at radial distances r_1 and r_2 respectively. Departing from the constitutive law

$$q_r = -\lambda \frac{dT}{dr}$$

and an assumption of how the radial heat flux varies with the radius:

$$q_r(\theta,r) = q_r(\theta,r_0)\frac{r_0}{r}$$

the expression:

$$\lambda(\theta,r_1,r_2) = -\frac{q_r(\theta,r_0)r_0}{T(\theta,r_1)\text{-}T(\theta,r_2)}\ln\frac{r_1}{r_2} \qquad (2)$$

is obtained. This expression is valid at mid height of and close to the canister. The expression is valid only for purely radial heat transport. Thus, the angle θ in Equation 2 does not indicate a directional dependence in the analytical expression it serves only as an indication of the position of the considered points. In the finite element model however, non-radial components of heat flux will be present due to the complex

geometry. The analytical expression is here considered a good approximation to the real situation and can give an indication of the magnitude of bentonite conductivity or, consequently, an estimate of the correctness of the heat flux.

The parameters are sampled at day 395 for the different holes. Below, the parameters and results are compiled in tables and schematic figures.

4.3.1 Hole 1

Table 4-1. Parameters for evaluation of bentonite thermal conductivity at day 395.

ID	A	B	C
θ [°]	0	90	180
r_1 [m]	0.585	0.585	0.585
r_2 [m]	0.685	0.635	0.685
$T(\theta, r_1)$ [°C]	69.1	68.8	69.4
$T(\theta, r_2)$ [°C]	62.7	66.0	63.7
$q_r(\theta, r_0)$ [W/m^2]	94.7	91.4	81.9
$\lambda(\theta, r_1, r_2)$ [W/(m·K)]	1.23	1.39	1.19

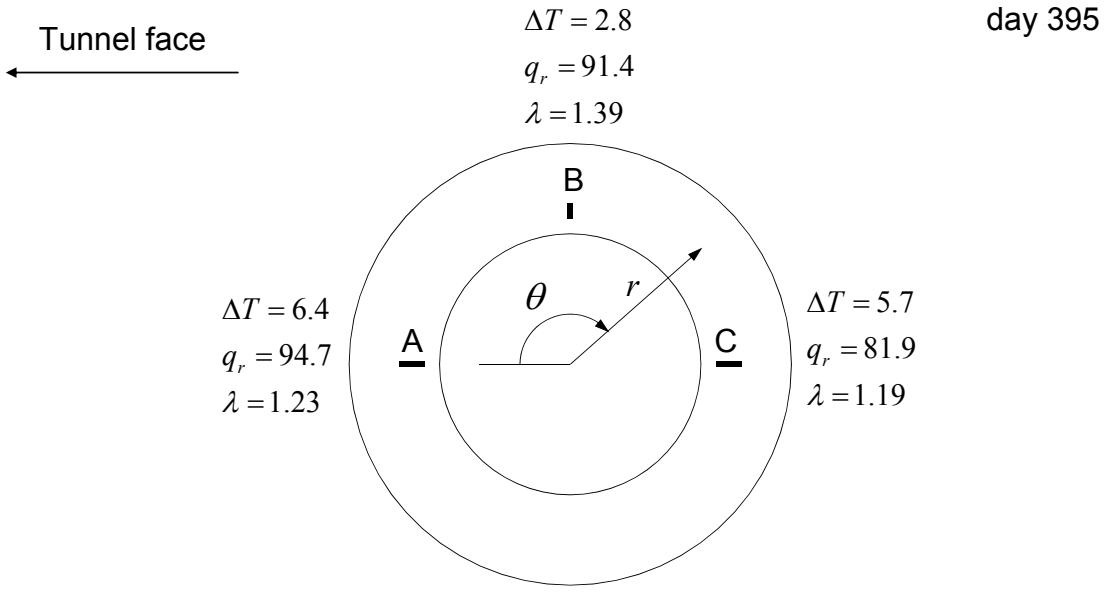

Figure 4-7. *Sensor positions and parameters at hole 1.*

The mean value of the calculated thermal conductivities is $\overline{\lambda} = 1.27$ W/(mK). The curve in Figure 4-8 shows that that the buffer has taken up enough water that the bentonite close to the canister has expanded and closed the 10 mm gap that existed initially between the canister and the bentonite blocks (i.e. no signs of a temperature drop close the canister surface, cf. corresponding results for hole #3 in Figure 4-11).

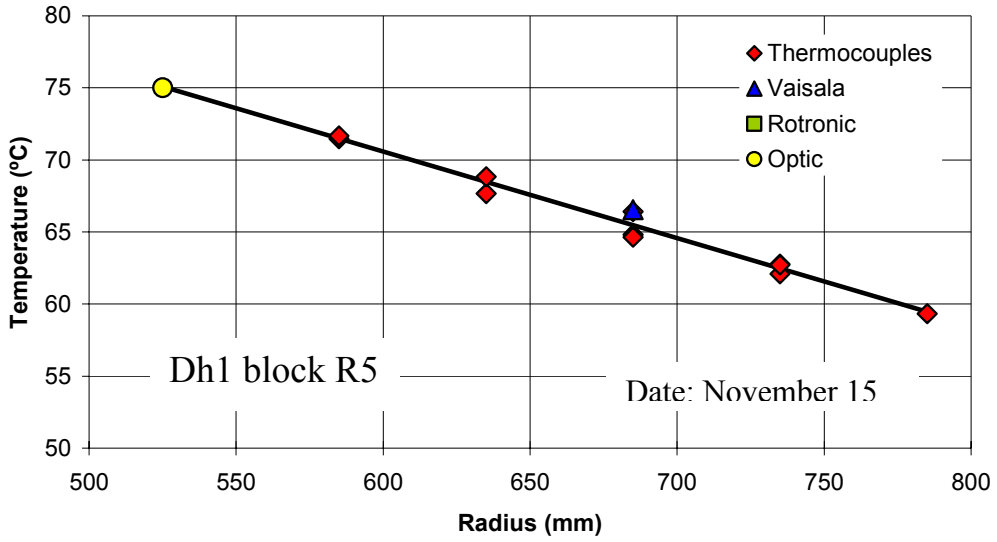

Figure 4-8. *The temperature in block R5 (canister mid-height) in Dh 1 as function of radius from the center of the deposition hole on November 15, 2004.From /Goudarzi and Johannesson, 2006/*

A comparison of the calculated mean value of the thermal conductivities with experimental data, see Figure 4-9, suggests that the bentonite is fully saturated or close to fully saturated, which agrees well with the observed characteristic of the temperature profile.

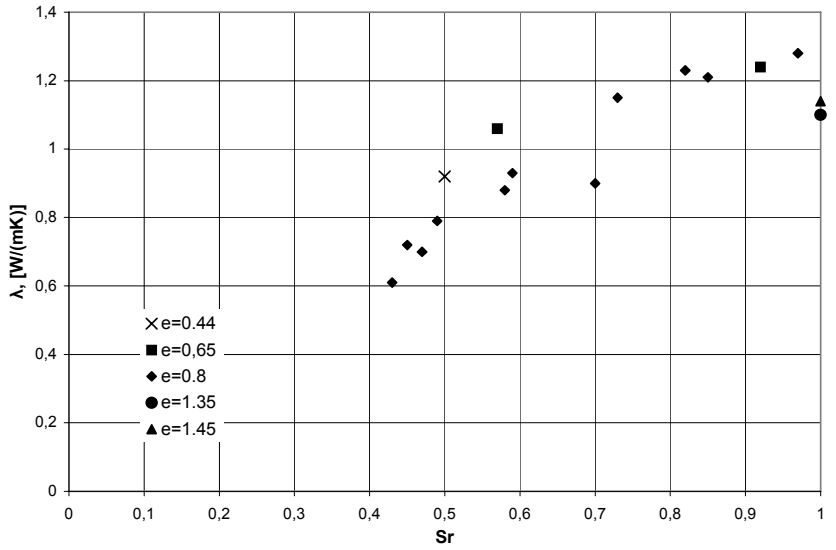

Figure 4-9. *Heat conductivity of MX80 bentonite as function of the degree of saturation. The legend gives the void ratio.*

4.3.2 Hole 3

Table 4-2. Parameters for evaluation of bentonite thermal conductivity at day 395.

ID	A	B	C
θ [°]	0	90	90
r_1 [m]	0.585	0.585	0.585
r_2 [m]	0.685	0.635	0.685
$T(\theta, r_1)$ [°C]	74.4	77.7	77.7
$T(\theta, r_2)$ [°C]	68.8	74.1	71.6
$q_r(\theta, r_0)$ [W/m^2]	87.4	91.1	91.1
$\lambda(\theta, r_1, r_2)$ [W/(m·K)]	1.29	1.09	1.24

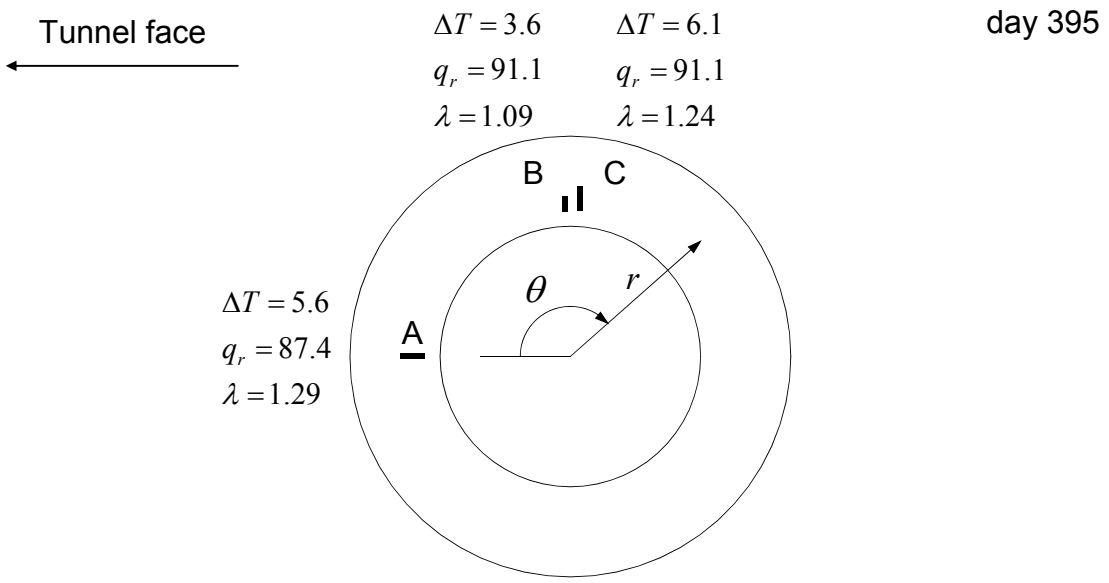

Figure 4-10. *Sensor positions and parameters at hole 3.*

The mean value of the calculated thermal conductivities is $\overline{\lambda} = 1.21\,\mathrm{W/(mK)}$. The temperature drop between canister and bentonite shown in Figure 4-11 indicates that the buffer has not taken up sufficient amounts of water to homogenize and close the open canister/bentonite gap. This verifies that hole 3 is dry as compared to hole 1.

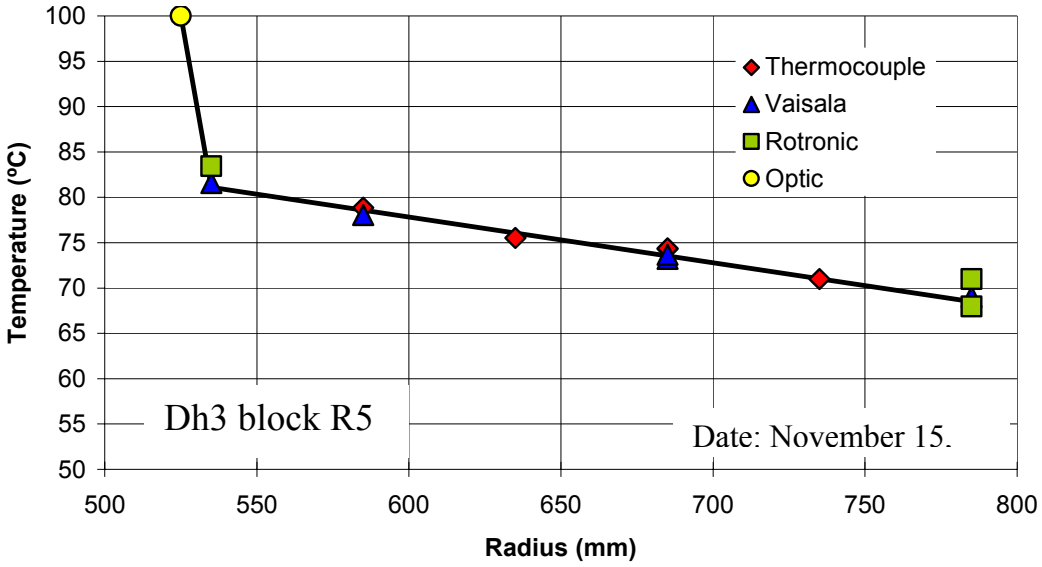

Figure 4-11. *The temperature in block R5 (canister mid-height) in Dh 3 as function of radius from the center of the deposition hole on November 15, 2004. From /Goudarzi and Johannesson, 2006/*

The lower mean value of thermal conductivity for hole 3 as compared to hole 1 indicates that the bentonite has not reached the same level of water saturation in hole 3.

If a linear dependence of thermal conductivity on water saturation is adopted, the bounds λ_{dry} = 0.3 W/(m·K) and λ_{wet} = 1.3 W/(m·K) seem appropriate when considering the calculated values of thermal conductivity for the two holes and the experimental measurements in Figure 4-9.

The thermal conductivity check also confirms that the calculated radial flux is appropriate both in magnitude, referring to the reasonable values of the calculated thermal conductivity as compared to the experimental measurements in Figure 4-9, and spatial representation, making the comparison of calculated thermal conductivity between the holes and the observed conditions for respective hole.

4.4 Rock temperatures

First the assumption of homogeneous thermal conductivity in the rock is evaluated for the base case by studying the temperature at corresponding points in the rock mass below the tunnel floor for each hole. Thereafter follow investigations of additional cases with different rock thermal conductivity, inhomogeneous conductivity and a decreasing background temperature. As a result of the study a relevant value of the effective rock conductivity is suggested. The recorded and simulated temperatures are then investigated close to hole 5 and hole 6. The character of the difference between the recorded and simulated temperatures is also studied.

4.4.1 Rock mass below tunnel floor

Base Case

Below follows an investigation of the validity of the assumption of homogeneous thermal conductivity in the rock for the base case. In Figure 4-12 and Figure 4-13 the rock temperature field at day 1171 is shown in a vertical plane in the tunnel direction and a horizontal plane 5 m below the tunnel floor respectively.

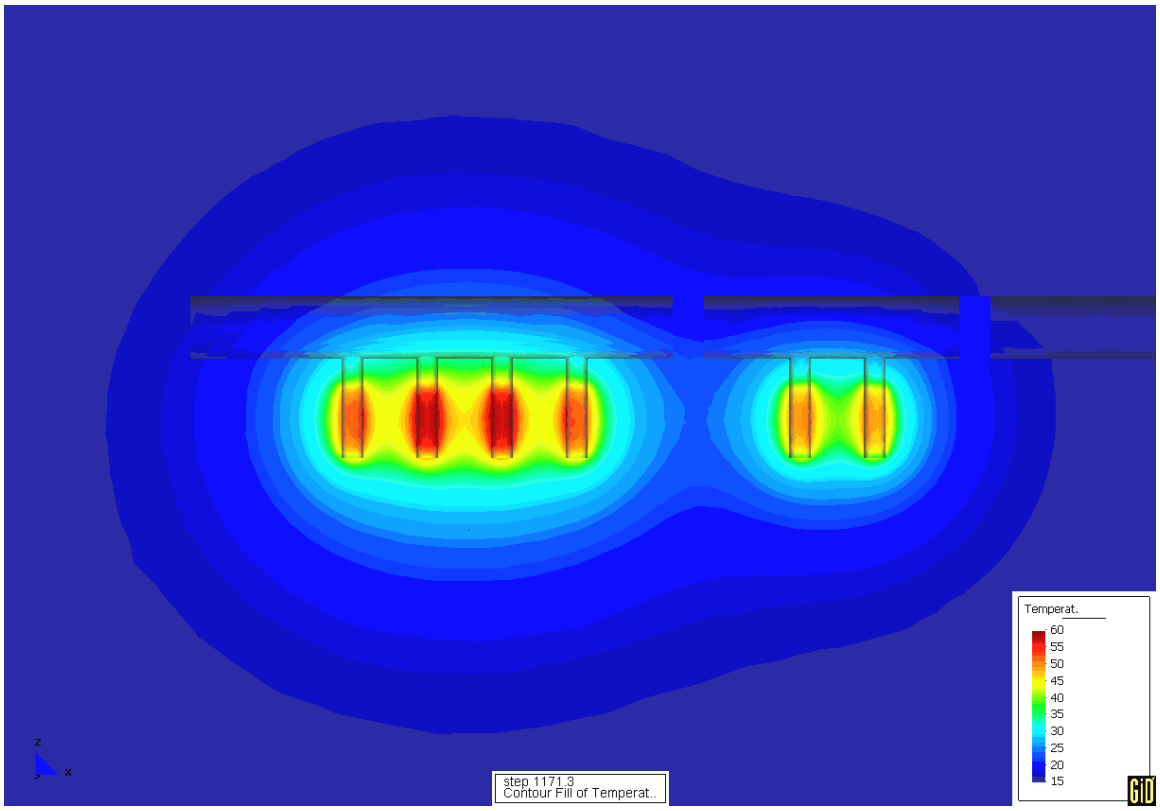

Figure 4-12 *The rock temperature shown in a vertical plane in the tunnel direction.*

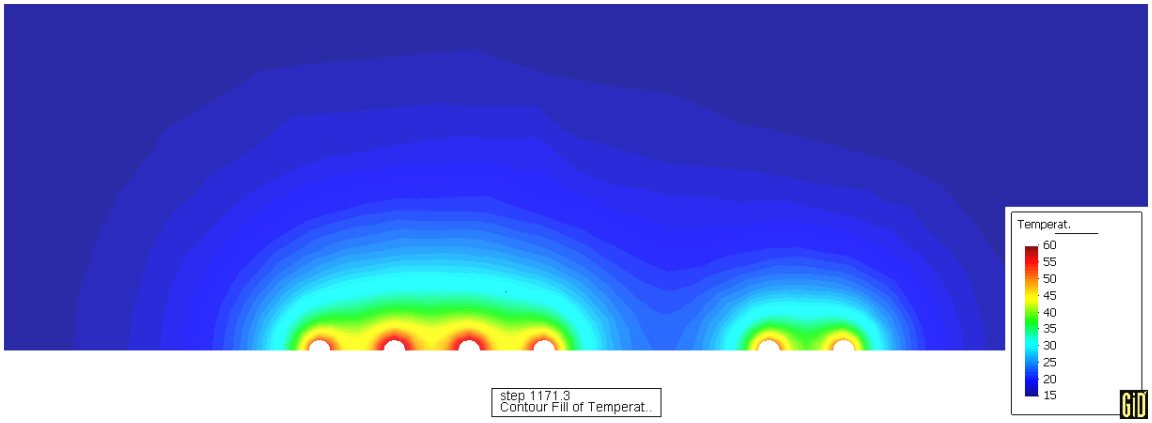

Figure 4-13. *The rock temperature shown in a horizontal plane at 5 m depth under the tunnel floor.*

Six points were selected for comparison between calculated and measured temperatures according to Figure 4-14. A compilation of computed and recorded temperatures at these points is shown below in Figure 4-15.

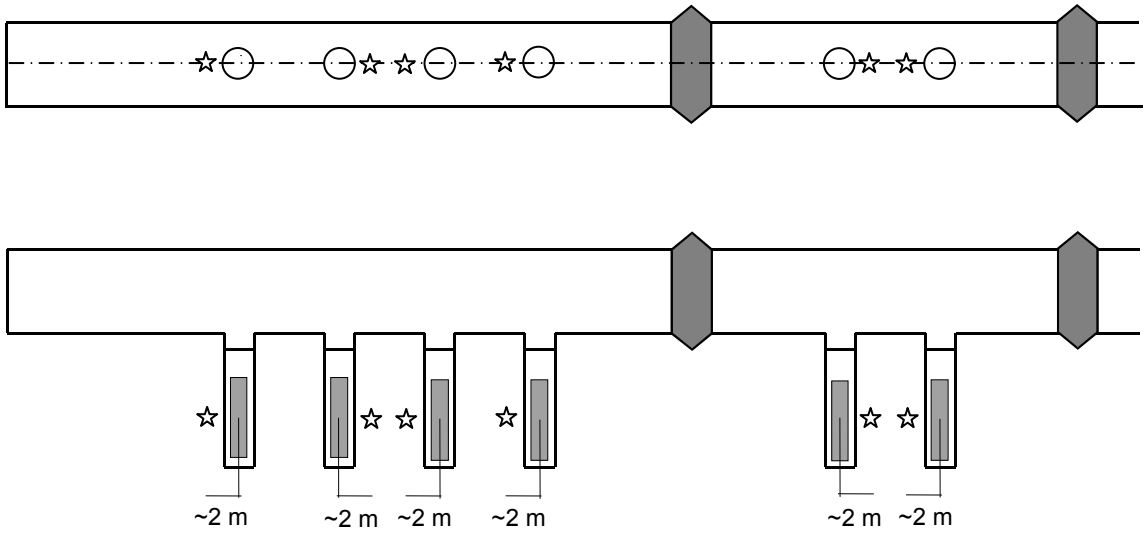

Figure 4-14. *Positions of sample points.*

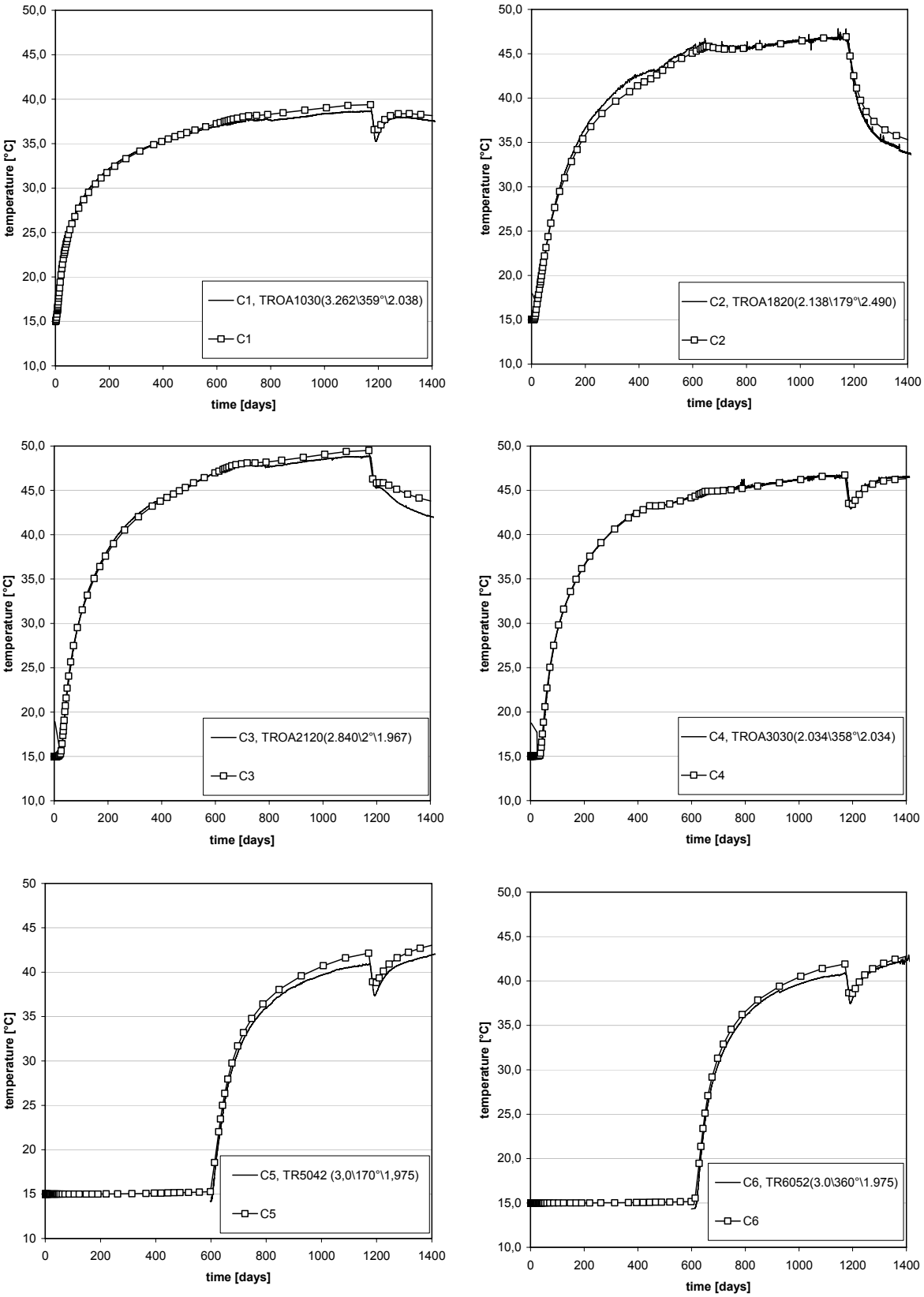

Figure 4-15. *Temperatures in sample points approx. at canister mid-height and 2 m from the canister axes, cf. Figure 4-14. Lines: measurements. The legend gives the sensor name and its position as given in the Prototype Repository data reports. Lines with symbols: corresponding calculated results.*

In Figure 4-15 and forthcoming figures, the letters and numbers besides the canister number in the legend indicates the sensor name and position according to the system used in /*Goudarzi R., Johannesson L-E., 2006*/.As Figure 4-15 shows, at the sample points the calculated temperature fits reasonably to the recorded ones in the pillars. This indicates that, as far as the thermal evolution at canister mid-height is concerned, the thermal conductivity of the prototype repository rock mass may well be approximated to be homogeneous.

Figure 4-16 shows the relative difference, $(\Delta T_{calc}/\Delta T_{exp}\text{-}1)100$ between the recorded and simulated base case temperature increase, $\Delta T_x = T_x - T_0$, where the x indicate that either experimental (exp) or calculated (calc) temperatures can be inserted. The relative difference is shown at times 190.9, 788.7 and 1171.3 days after test start. Note that at 190.9 days heaters 5 and 6 are not yet in operation. The relative difference never exceeds 5 % in the base case. The relative differences have an overall trend towards increasing in the positive direction, i.e. the calculations tend to overestimate the temperatures (except for canister 4).

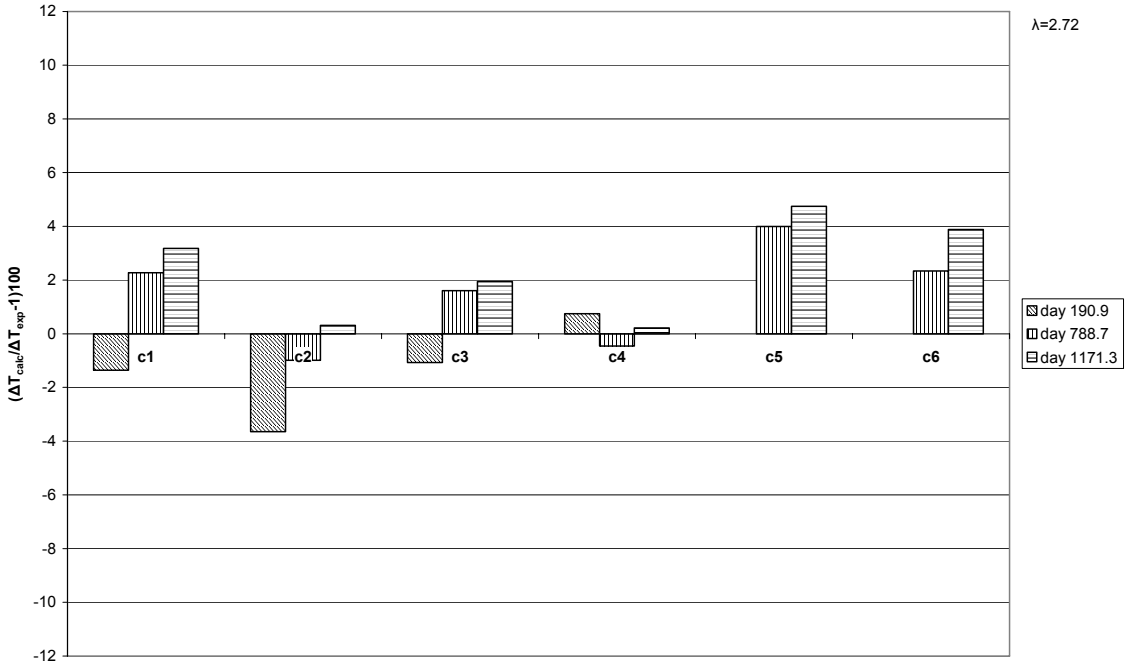

Figure 4-16. *Relative difference diagram of the base case.*

Additional cases

Here cases where properties have been altered as compared to the base case are studied.

It has been suggested in /Sundberg et al 2005/ that a slow global decrease in background temperature could be present in the area close to the experimental site. This comes from the heating produced when excavating the tunnel and holes and installing the experimental equipment. To illustrate the impact of this on the rock temperature an assumption of -0.2 °C/year, as suggested in /Sundberg et al 2005/ was adopted. The results were obtained by processing the data obtained from the base case simulation.

An investigation in /Sundberg et al 2005/ showed that in order to back-calculate the rock temperatures close to the tunnel floor well, the rock thermal conductivity had to be increased in the floor region as compared to the overall value. This is probably an effect of water movement in the rock closest to the pressure-controlled backfilled tunnel, i.e. not a true difference in thermal conductivity. Here the tunnel floor, an annular 1 m thick region, see Figure 4-17, was given a thermal conductivity of λ = 3.5 W/(m·K) in order to account for this.

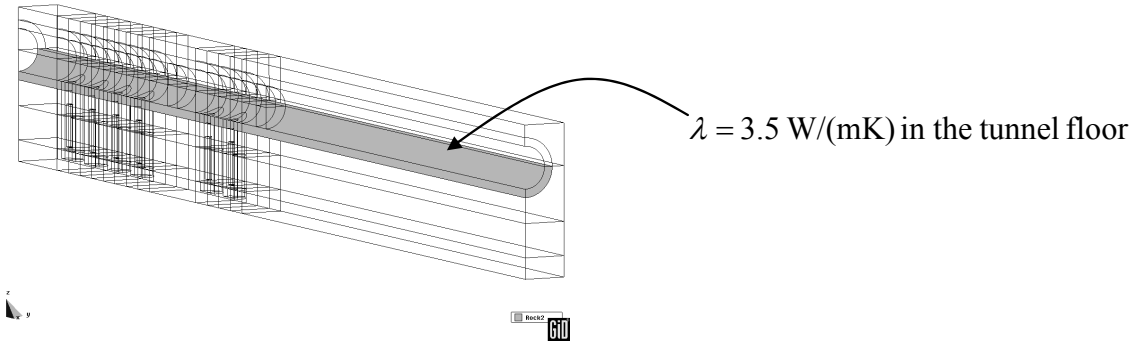

Figure 4-17. *Tunnel floor geometry.*

The rock conductivity has also been altered to λ = 2.65 W/(m·K) and λ = 2.52 W/(m·K). These values has been taken from /Sundberg et al 2005/. The first value, λ = 2.65 W/(m·K), corresponds to that obtained from the inverse modeling in /Sundberg et al 2005/ where the global decrease of the background temperature change is included and sensors indicating values above 3.4 W/(m·K) have been disregarded. For more information about the inverse modeling see /Sundberg et al 2005/. The second value, λ = 2.52 W/(m·K), was obtained as the mean of laboratory measurements on samples taken from both Prototype Repository sections.

For each of the three rock conductivity choices there are four different cases, 1) the plain case as in the base case above, 2) the case where the global temperature change is considered, 3) the case where the tunnel floor conductivity is altered and 4) the case where both global temperature change and changed floor conductivity are considered. This makes twelve different cases in total, cf. Table 3-2. The corresponding diagrams are shown in Appendix 1.

Here, the information of the twelve diagrams has been condensed into one single diagram showing the mean value and standard deviation of the relative differences for each of the twelve cases. As seen in Figure 4-18 there are two columns for each case, one representing the mean value and one representing the standard deviation.

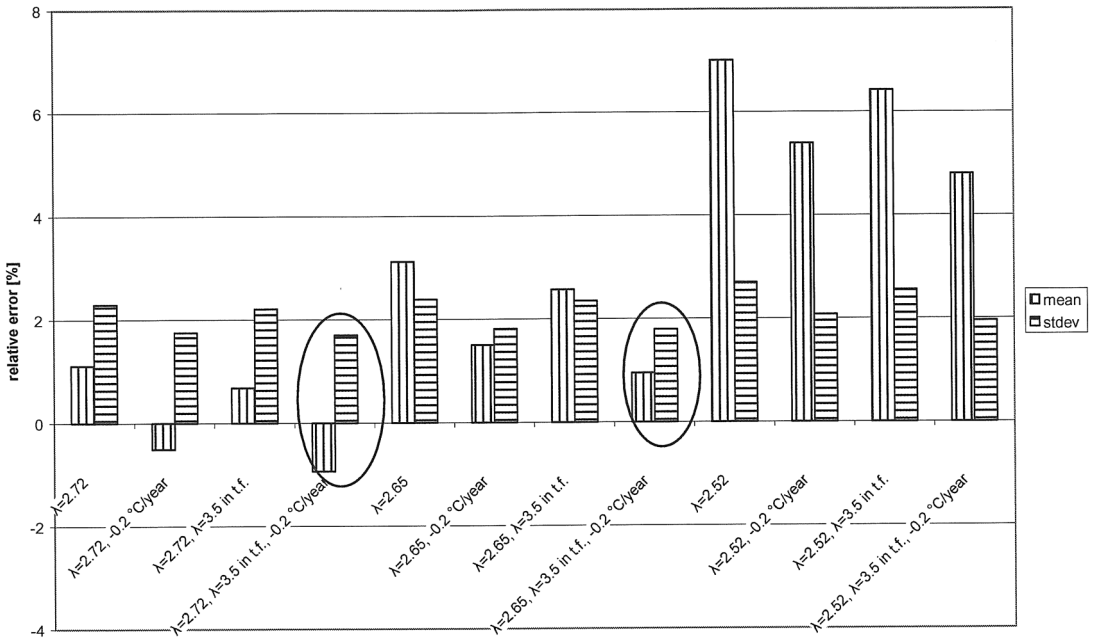

Figure 4-18. *Mean values and standard deviations of relative error found in cases 1-12. Positive mean values mean that the calculations overestimate the measured ones (i.e. average of the six sampling points) Out of the 12 cases the two marked by ellipses were selected to define an additional one, see text below.*

If the cases where both the global temperature change and the change in the tunnel floor conductivity are considered the most relevant, the simulations marked with ellipses in Figure 4-18, where λ = 2.72 W/(m·K) and λ = 2.65 W/(m·K), can be considered to be the best. If a linear dependence of the mean value on the heat conduction is assumed, the best fit in terms of mean value is obtained for λ = 2.685 W/(m·K). The compilation of computed and recorded temperatures and resulting relative difference column diagram for λ = 2.685 W/(m·K) are shown in Figure 4-19 and Figure 4-20 respectively. The mean value of -0.04 % and standard deviation of 1.77 % indicates that the chosen heat conductivity represents the temperature field well.

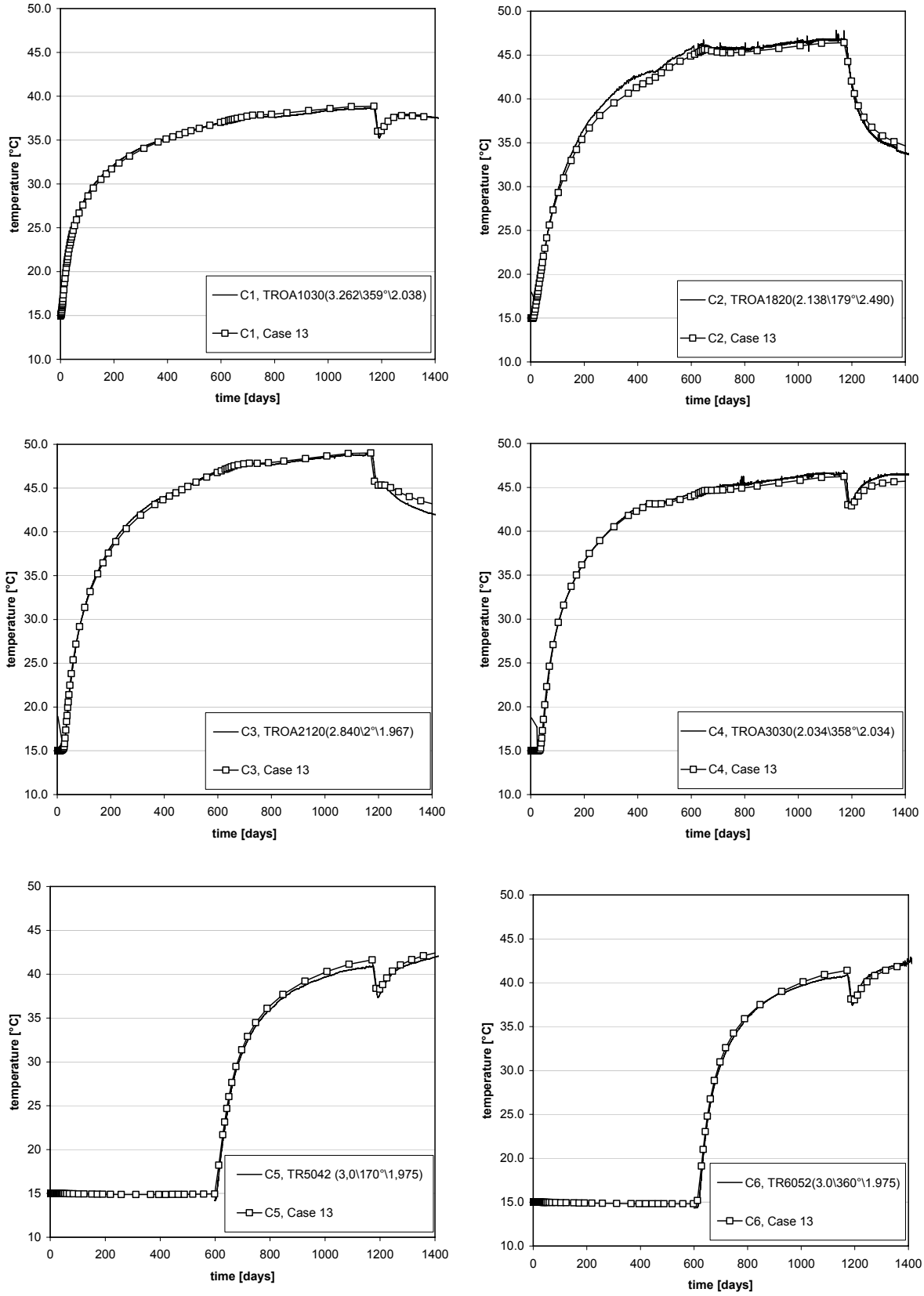

Figure 4-19. *Temperatures in sample points approx. at canister mid-height and 2 m from the canister axes, cf. Figure 4-14. Lines: measurements. The legend gives the sensor name and its position as given in the Prototype Repository data reports. Lines with symbols: corresponding calculated results.*

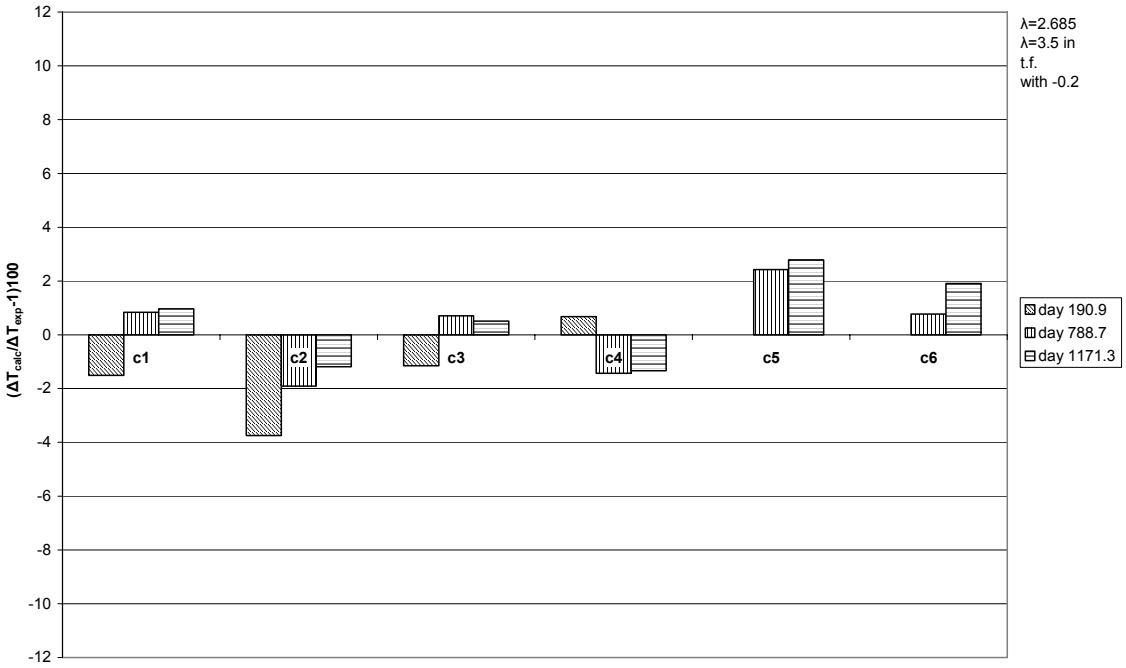

Figure 4-20. *Relative difference block diagram of the case where λ = 2.685 W/(m·K), the tunnel floor has an increased heat conductivity of 3.5 W/(m·K) and a global background temperature 0.2 degr/yr decrease is considered.*

4.4.2 Temperatures in the walls of hole 5 and hole 6

A closer study of the rock temperatures can be interesting when evaluating the difference between experiment and simulation. The two holes in the outer section (5 and 6) are more extensively instrumented than the four holes in the inner section. There are, for instance, a number of thermocouples in the walls of these holes. Figure 4-21 and Figure 4-22 show measured temperatures and temperatures obtained from what appears to be the best model out of those considered here (i.e. the one with λ = 2.685 W/(m·K) for the rock mass, increased conductivity in the tunnel floor and with a 0.2 °C/year decrease of the background temperature). Filled symbols mean measured temperatures and empty symbols calculated temperatures. Note that some of the results (thermocouples TR5042 and TR6052 and corresponding calculated results) are identical to those found in Figure 4-15.

The black dots in the insets show the instrument positions; white dots show the mesh grid-points used for the comparison. For the instrument positions closest to the walls (distance 200mm), the calculated evolution was obtained by interpolation between neighboring gridpoints.

The temperatures at the smallest distance seem to be underestimated by between 0.5 ºC and 2 ºC. At the hottest points (indicated with circles) the underestimate is between 0.5 ºC and 1.0 ºC. It is not clear if this small underestimate is systematic, i.e. if the conductivity value found to be generally relevant to the temperature evolution in the pillars (cf. Figure 4-19) would be too high to capture the rock wall temperatures. To find out if the underestimate is systematic it would to be useful to have measurements from points at the walls also from 1-4 (i.e. not just from the few positions in holes 5 and 6).

It should be noted too, however, that the rock wall temperatures (at individual rock wall points) are sensitive to the local heat flux distribution which can be affected by uneven water uptake and, possibly, by misalignment of the canisters in the deposition hole. In addition there is the influence of non-linearity (i.e. the rock thermal conductivity is slightly decreased in the hottest rock).

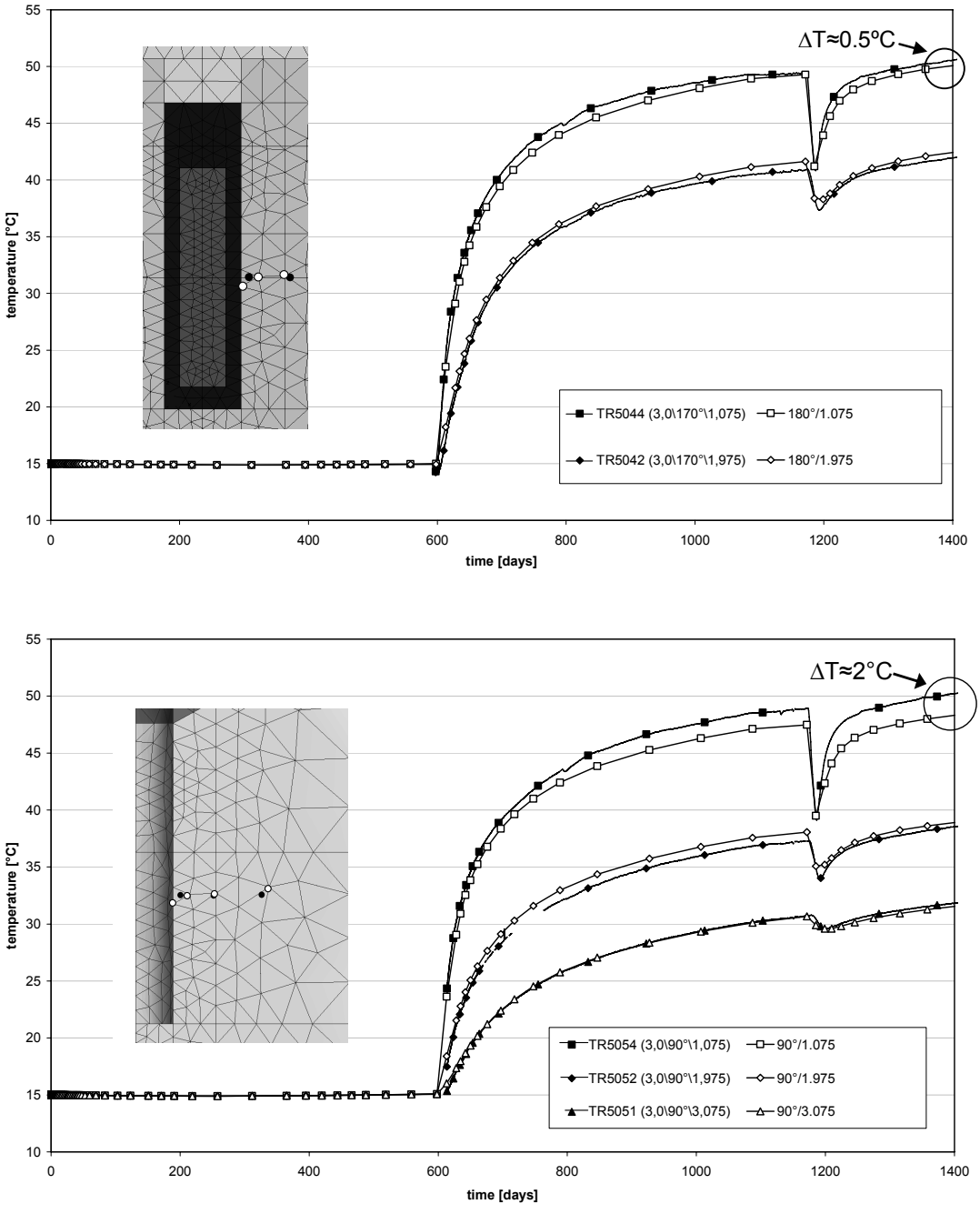

Figure 4-21. *Rock temperatures close to hole 5. Comparison between measured (filled symbols) and calculated (empty symbols) Case 13 temperatures. Upper: Positions along tunnel axis. Lower: Positions 90º off axis.*

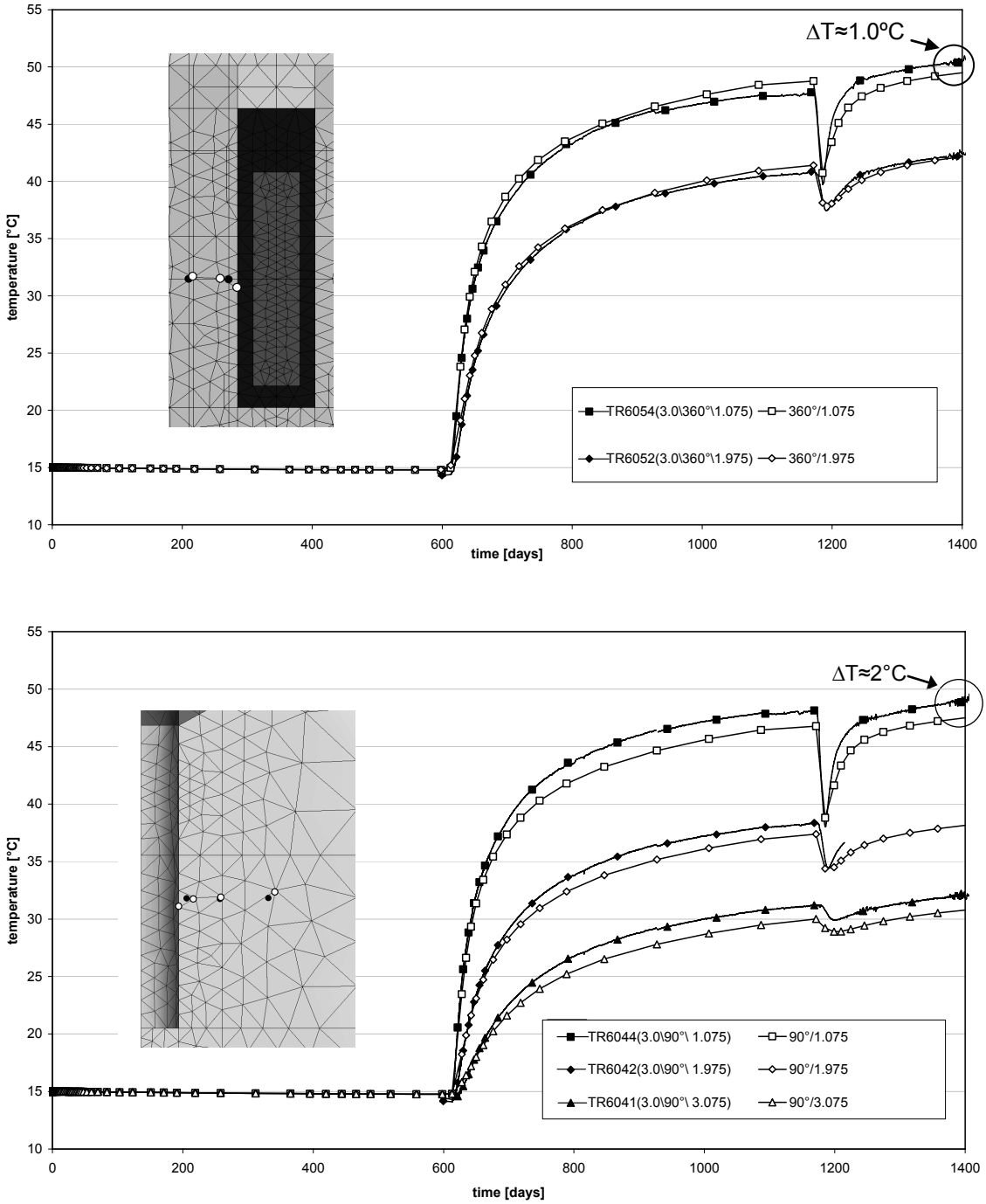

Figure 4-22. *Rock temperatures close to hole 6. Comparison between measured (filled symbols) and calculated (empty symbols) Case 13 temperatures. Upper: Positions along tunnel axis. Lower: Positions 90º off axis.*

Figure 4-23 shows the calculated and measured maximum temperatures found in the two previous figures, now compared with the corresponding Case 12 temperatures (rock conductivity 2.52 W/(m·K), increased floor conductivity to 3.5 W/(m·K), and 0.2 ºC/year decrease in background temperature, cf. Table 3-2). The two calculated results seem to bracket the measured results very tightly.

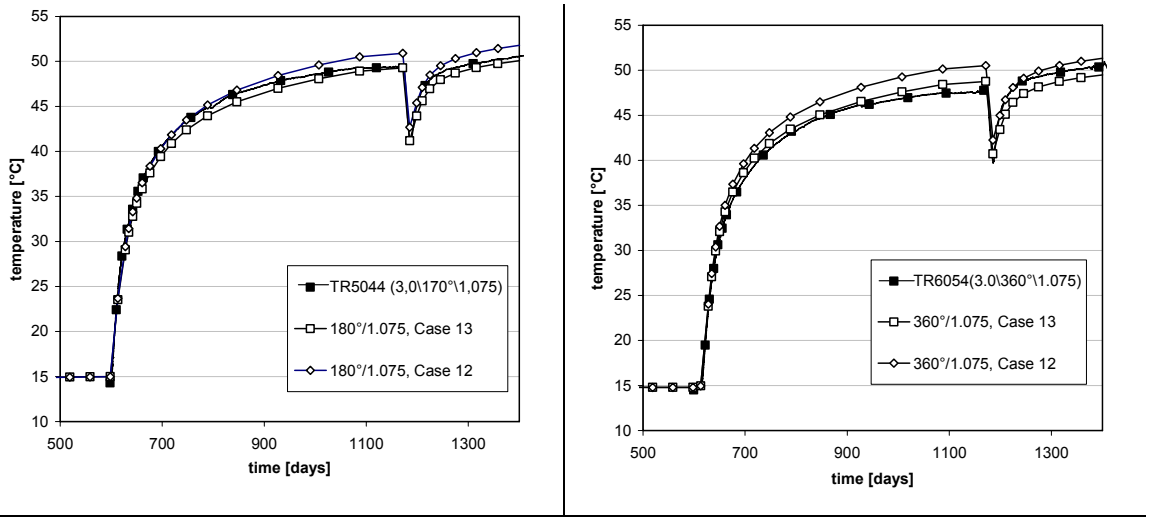

Figure 4-23. *Measured temperatures (filled symbols) 200 mm from rock wall in hole 5 (left) and hole 6 (right) compared with corresponding calculated Case 12 and Case 13 results (empty symbols).*

4.5 Backfill thermal conductivity analysis

In this analysis the backfill were given different values of thermal conductivity as compared to the base case in order to study the influence on rock wall temperature at the mid-height of the buffer and on the temperature above the canister. In the base case the backfill was given a thermal conductivity of λ = 1.5 W/(m·K) and in the two additional cases λ = 1.0 W/(m·K) and λ = 2.72 W/(m·K), which corresponds to the values adopted for buffer and rock, respectively. The resulting responses are shown in Figure 4-24 and Figure 4-25.

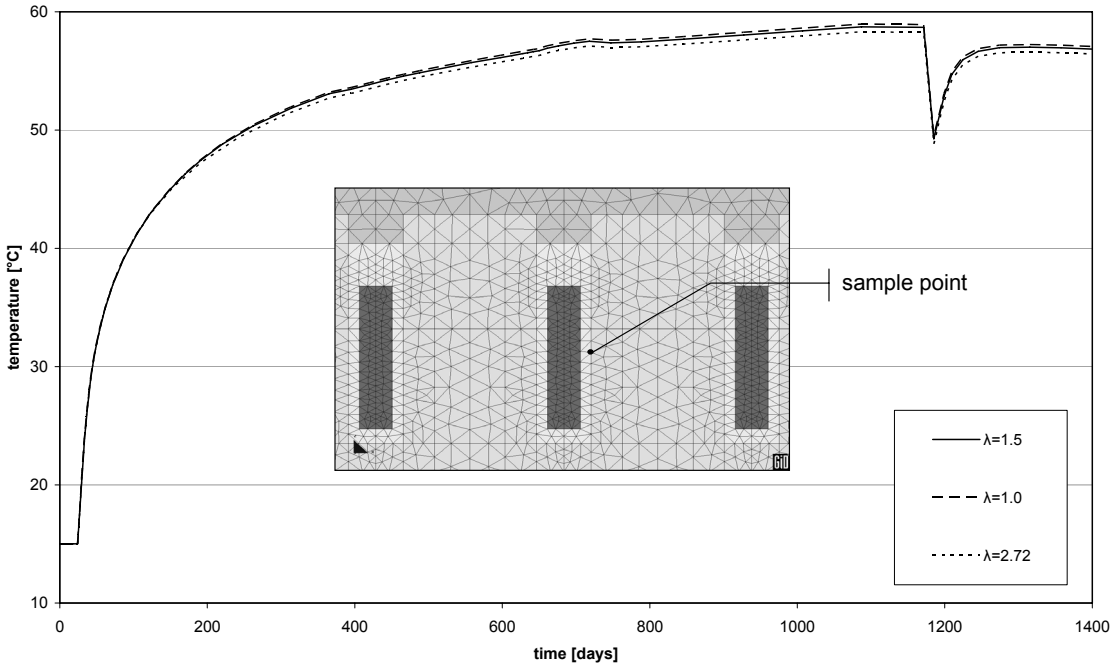

Figure 4-24. *Temperature at buffer/rock interface when changing thermal conductivity of the backfill.*

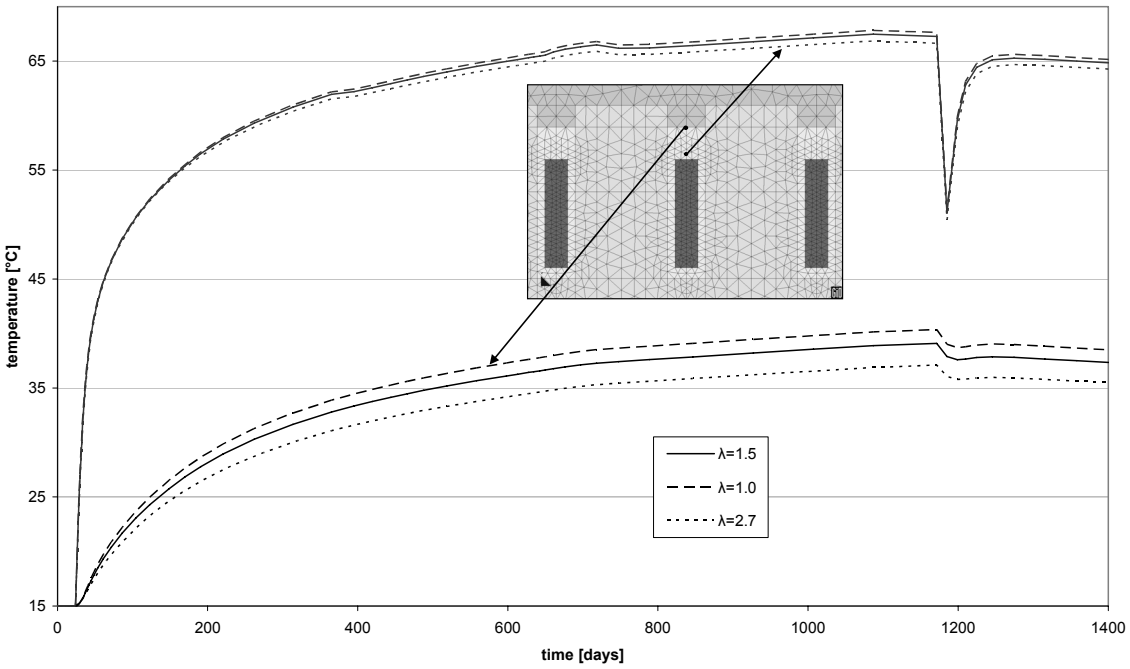

Figure 4-25. *Temperature above the canister when changing thermal conductivity of the backfill.*

It can be seen in Figure 4-24 that the temperature at the buffer/rock interface at canister mid height is not significantly affected by the change in backfill thermal conductivity for the conditions that prevail in this model. The temperature above the canister is significantly affected at the backfill/bentonite-block interface. Closer to the canister the influence is not significantly influenced by the changed backfill property.

4.6 Tunnel convection analysis

Here the boundary conditions of the part of the tunnel which is not filled were changed from adiabatic, which were adopted in the base case, to account for cooling by convection. A convection heat transfer coefficient of γ = 10 W/(m^2·K)were used.

Figure 4-26 and Figure 4-27 show isotherms around hole 5 and hole 6 for the two different tunnel conditions. The apparent discontinuities in the isolines only come from that the backfill has been excluded in the post-processing in order to reveal the rock temperatures.

When comparing the isolines in the figures it can be seen that the different tunnel conditions gives slightly different temperature fields. The convective conditions affect the temperature field around hole 6, the right hole in the figures, by lowering the temperatures at the side facing the open tunnel. Close to the canister, the effect is insignificant. The temperatures around hole 5, the left hole, are hardly affected by the tunnel conditions at all.

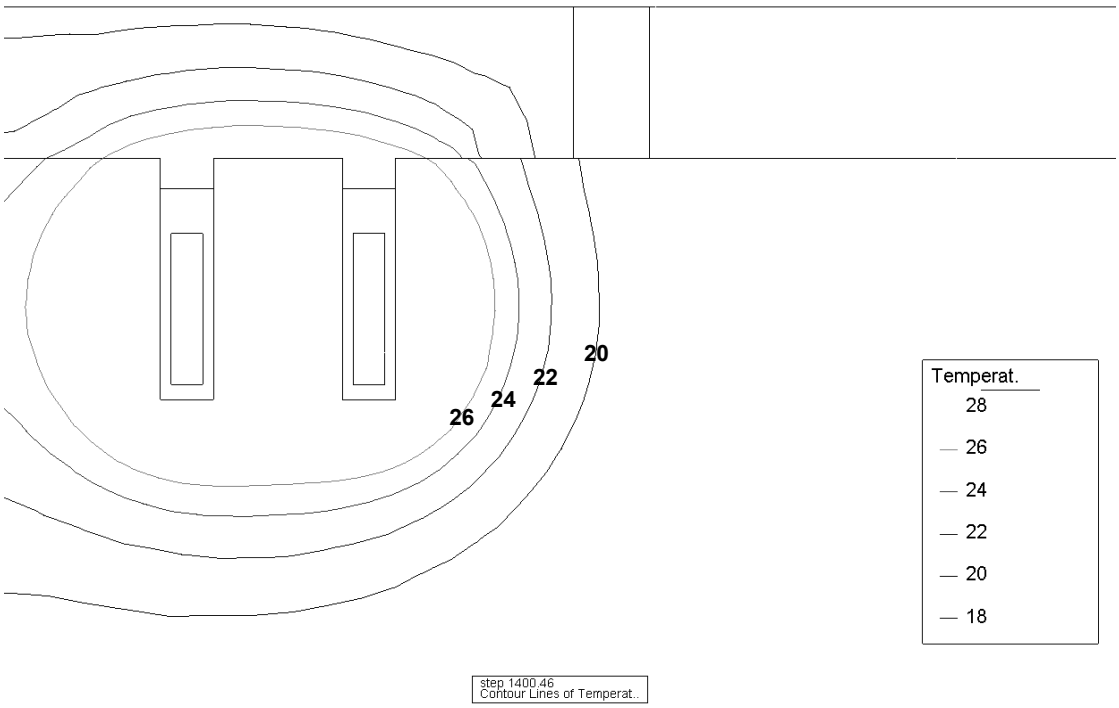

Figure 4-26. *Contour lines of temperature around hole 5 and hole 6 with adiabatic tunnel conditions.*

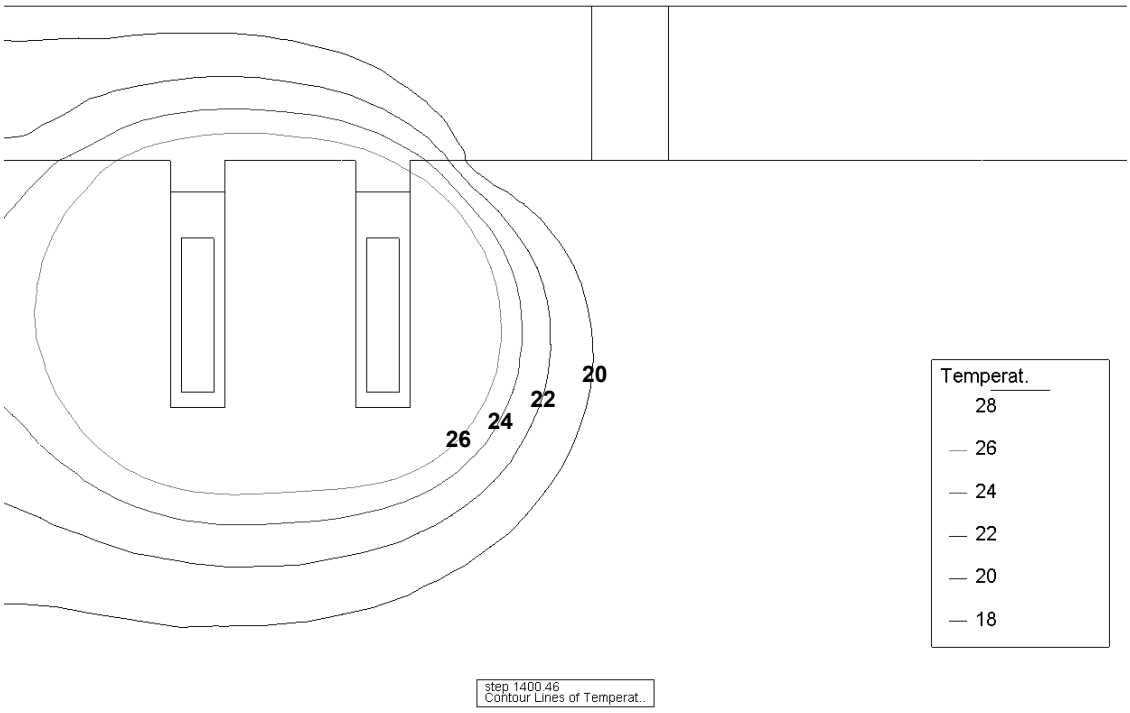

Figure 4-27. *Contour lines of temperature around hole 5 and hole 6 with tunnel convection.*

5 Conclusions and discussion

5.1 Thermal boundary conditions for local THM models

Two time-dependant boundary conditions are required for local THM models: the heat flux at the canister surface and the temperature at the wall of the deposition hole. Both conditions can be obtained, for each of the six Prototype Repository deposition holes, from the files generated by the simulations reported here.

- The agreement between measured and calculated rock temperatures verifies that the load histories of the different canisters are valid.
- The agreement between thermal bentonite conductivities measured in the laboratory and those derived here from measured bentonite temperatures and calculated heat fluxes indicates that the heat fluxes are valid. Disturbances caused by asymmetry and, possibly different rates of water uptake in different azimuths, are sufficiently small that the assumption of idealized radial symmetric heat fluxes will be relevant when defining boundary conditions.
- Calculated and measured temperatures at the walls of the different deposition holes could be compared only for the extensively instrumented holes 5 and 6, but again, the general agreement between calculated and measured temperatures at other points suggests that the rock wall temperatures calculated for all holes would be valid boundary conditions.

5.2 Rock thermal conductivity

The following observations are made:

- Numerically it appeared to be possible to reproduce the recorded temperature evolution close to all six canisters some 5 m below the tunnel floor well using one discrete global value of the rock mass thermal conductivity (although conductivity determinations made on laboratory-scale samples from the Prototype Repository Rock mass indicate that there may be a significant variability, cf. for instance Figure 5-1). No difference larger than 2 ºC was found for the base case (λ=2.72 W/(m·K)); the average differences were much smaller (cf. Figure 4-15 and Figure 4-16).
- Reducing the thermal conductivity by 0.035 W/(m·K) and accounting for an apparent decrease of the background temperature (estimated at 0.2 Cº/year /Sundberg et al., 2005/) and for enhanced heat transport in the floor region (probably associated with water movements below the drained backfill) increased the average precision (cf. Figure 4-19 and Figure 4-20).
- The value 2.52 W/(m·K) which is suggested as the best prognosis /Sundberg et al, 2005/ and was based on lab test results gives a general overestimate of the temperatures. This is true even accounting for the excess conductivity in the floor and for a decreasing background temperature (cf. Appendix 1, Figs 7-9 through 7-12).

The above shows that λ= 2.7 W/(m·K) probably is a relevant effective thermal conductivity value for the Prototype Repository rock mass. However, for the six pillar points being particularly analyzed here (cf. Figure 4-14), small-scale spatial variability is not as important as it might be for points at the walls of the deposition holes. The temperature evolution at the six pillar points is determined by properties averaged over larger volumes (at least the volume of the pillar between the two closest heat sources, i.e. 30-50 m^3) than the volumes that dominate the evolution at specific wall points (probably 1-5 m^3). In addition there are the possible effects of non-linearity; i.e. there may be a small conductivity reduction in the hottest parts of the rock, i.e. in the wall regions. This means that one could not necessarily expect calculated and measured rock wall temperatures to match as well as the pillar temperatures.

Unfortunately, there are no temperature sensors in the walls of any deposition holes other than nr 5 and nr 6. Therefore it is not possible to check with any rigor if the effective value 2.7 W/(m·K) would reproduce the temperatures at the walls of the deposition holes as well as it reproduced the temperatures at the six specific pillar points. The results shown in Figure 4-21 and Figure 4-22 for points at the walls of holes nr 5 and nr 6 indicate that this is almost, but not exactly, the case: out of the four sensor points, the agreement is very good for one point whereas the model underestimated the measured temperature by 1.5 - 2 ºC for the other three. The results in Figure 4-23 show that the best prognosis value 2.52 W/(m·K) /Sundberg et al., 2005/, (i.e. case 12) would be too low to reproduce the measured rock wall temperatures. This suggests that a Prototype Repository rock mass thermal conductivity of 2.6 W/(m·K) would be needed in the model to reproduce the temperatures at the walls of Prototype Repository deposition holes.

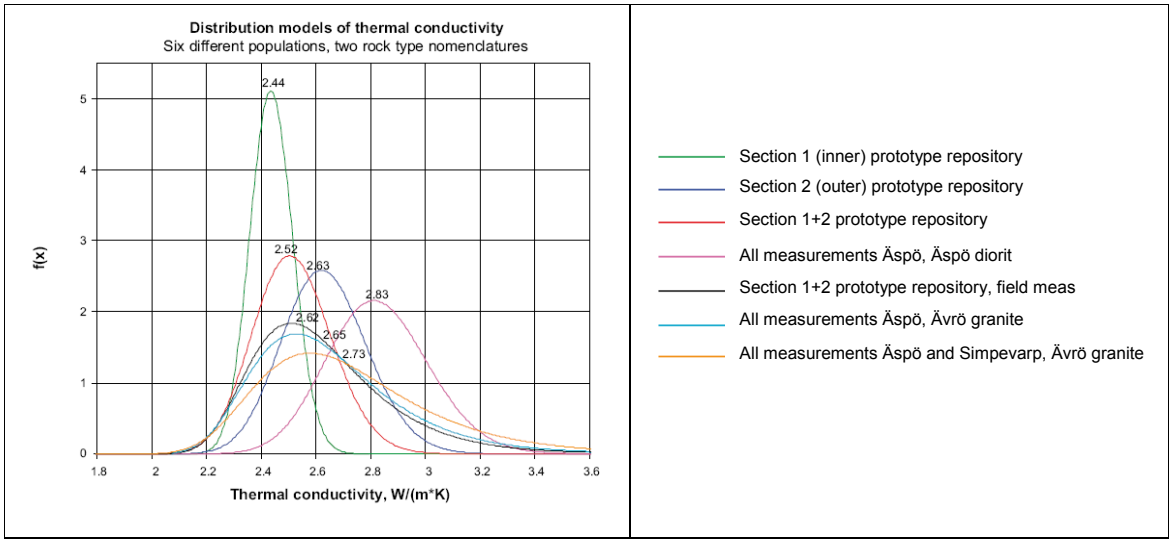

Figure 5-1*. Conductivity distributions suggested for the Prototype Repository rock mass. From /Sundberg et al., 2005/*

5.3 Backfill thermal conductivity

The temperature at the buffer/rock interface at canister mid height was not significantly affected by a changing the backfill thermal conductivity within the range 1.0 - 2.72 W/(m·K) (cf. Figure 4-24). This in agreement with previous results, see e.g. /Hökmark and Fälth, 2003/. This holds true also for the temperature in the region around the top of the canister (cf. Figure 4-25).

5.4 Tunnel convection

When incorporating tunnel convection in the model, i.e. accounting for the ventilation outside the confining plug, the temperature field just inside the plug was moderately influenced. The effects on the temperatures calculated close to the deposition holes were insignificant.

6 References

Börgesson L. Hernelind J., 1999, Coupled thermo-hydro-mechanical calculations of the water saturation phase of a KBS-3 deposition hole. Influence of hydraulic rock properties on the water saturation phase. TR-99-41.

Börgesson L, Gunnarsson D, Johannesson L-E, Sandén T, 2002. Prototype Repository, Installation of buffer, canisters, backfill and instruments in Section 1. SKB IPR-02-23. Svensk Kärnbränslehantering AB

Fälth B., Kristensson O., Hökmark H., 2005, Äspö Hard Rock Laboratory, Äspö Pillar Stability Experiment, Thermo-mechanical 3D back analyze of the heating phase. IPR-05-19.

Goudarzi R., Johannesson L-E., 2006. Äspö Hard Rock Laboratory. Prototype Repository. Sensors Data Report (Period 010917-060601) Report No: 15. SKB IPR-06-26.

Hökmark H, Fälth B, 2003. Thermal dimensioning of the deep repository. Influence of canister spacing, canister power, rock thermal properties and nearfield design on the maximum canister surface temperature. SKB TR-03-09.

Sundberg J, Back P, Hellström G, 2005. Scale dependence and estimation of rock thermal conductivity. Analysis of upscaling, inverse thermal modeling and value of information with the Äspö HRL Prototype Repository as an example. SKB-R-05-82.

SKB, 2004. Deep repository. Underground design premises. SKB R-04-60.

7 Appendix 1

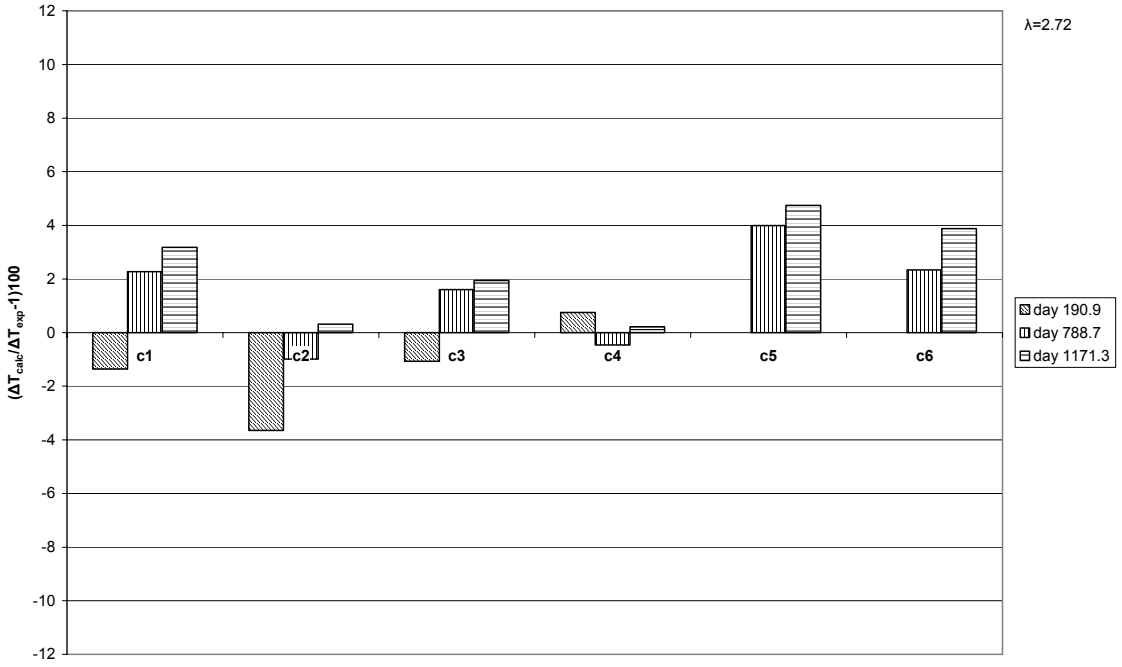

Figure 7-1. *λ = 2.72 W/(m·K)*

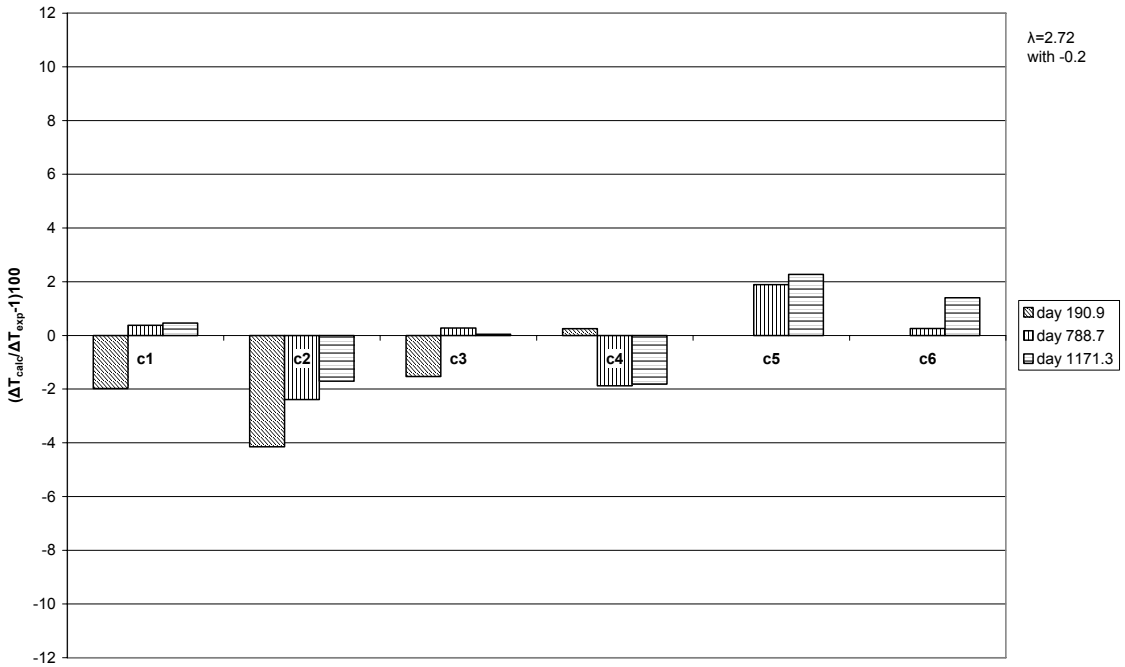

Figure 7-2. *λ = 2.72 W/(m·K), background temperature reduction.*

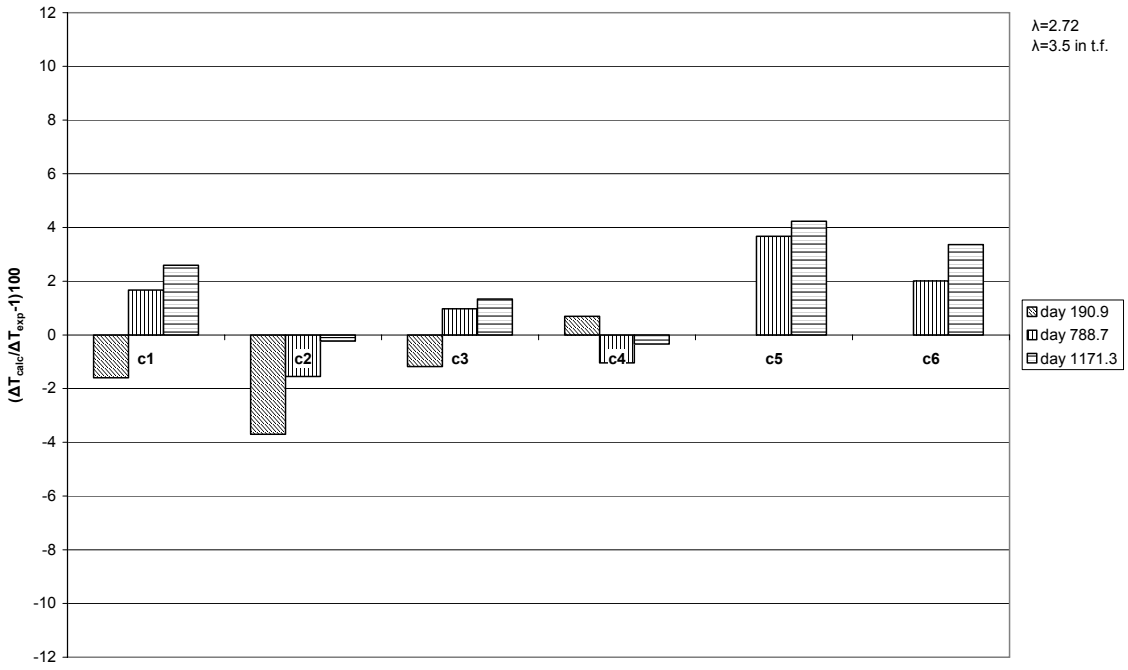

Figure 7-3. *λ = 2.72 W/(m·K), tunnel floor thermal conductivity 3.5 W/(m·K).*

Figure 7-4. *λ = 2.72 W/(m·K), background temperature reduction, tunnel floor thermal conductivity 3.5 W/(m·K).*

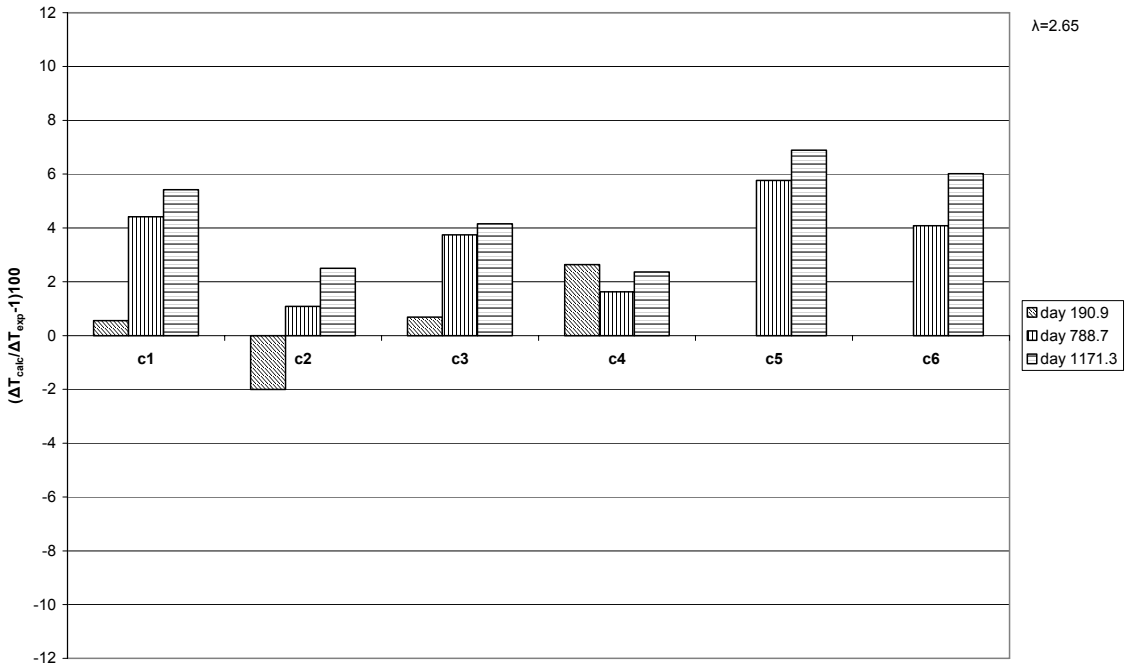

Figure 7-5. *λ = 2.65 W/(m·K).*

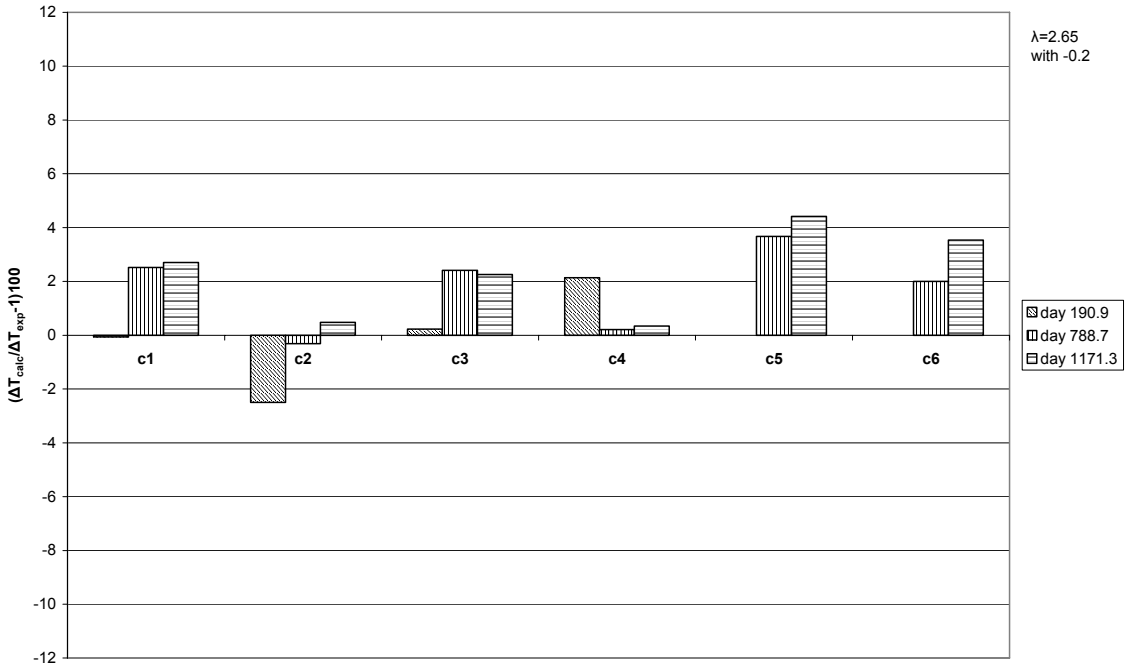

Figure 7-6. *λ = 2.65 W/(m·K), background temperature reduction.*

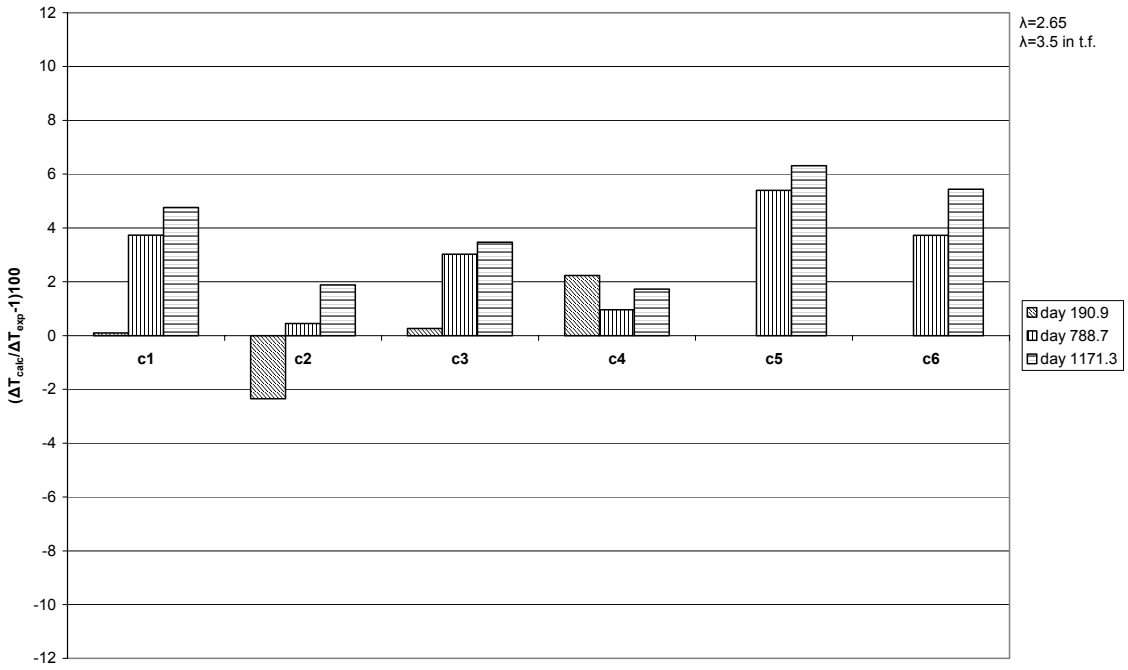

Figure 7-7. *λ = 2.65 W/(m·K), tunnel floor thermal conductivity 3.5 W/(m·K).*

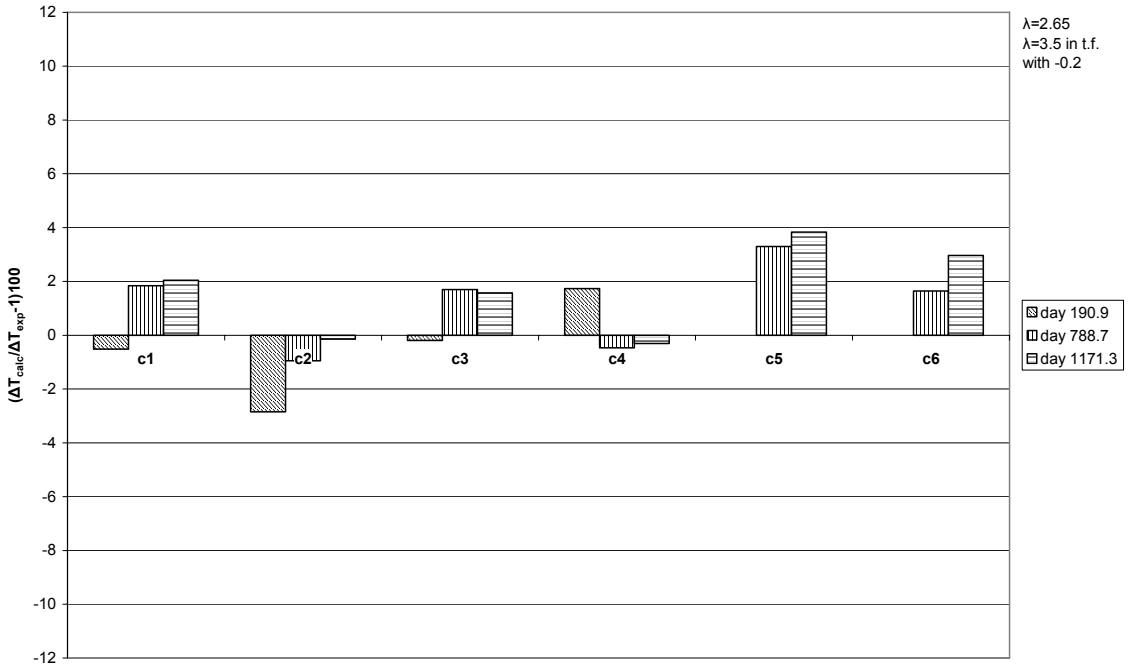

Figure 7-8. *λ = 2.65 W/(m·K), background temperature reduction, tunnel floor thermal conductivity 3.5 W/(m·K).*

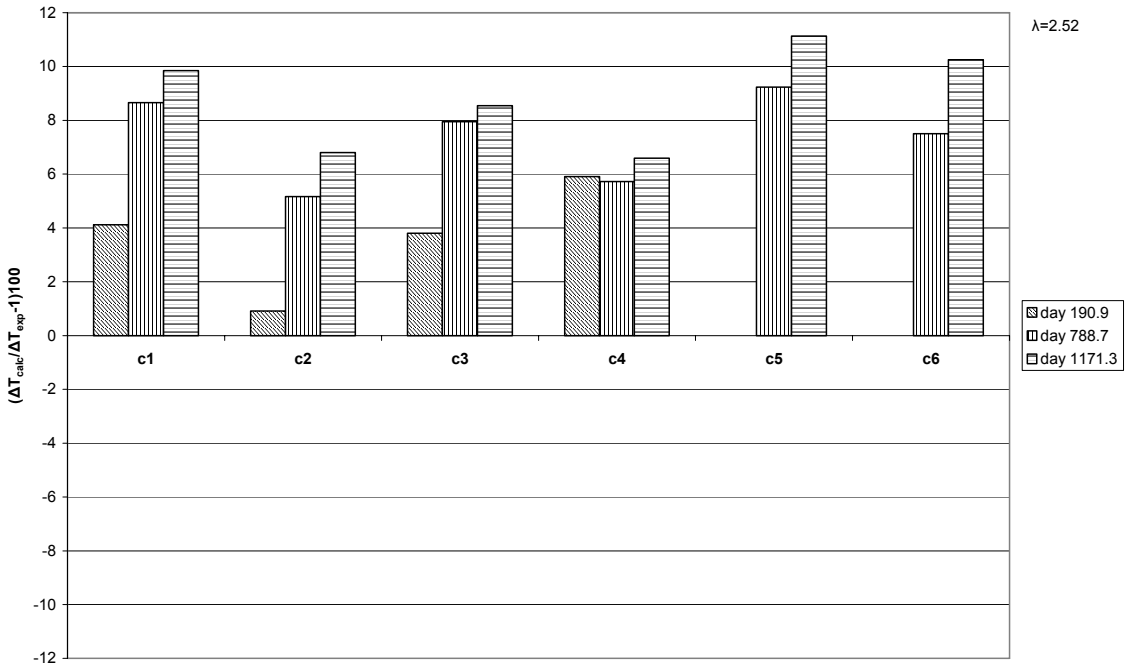

Figure 7-9. *λ = 2.52 W/(m·K).*

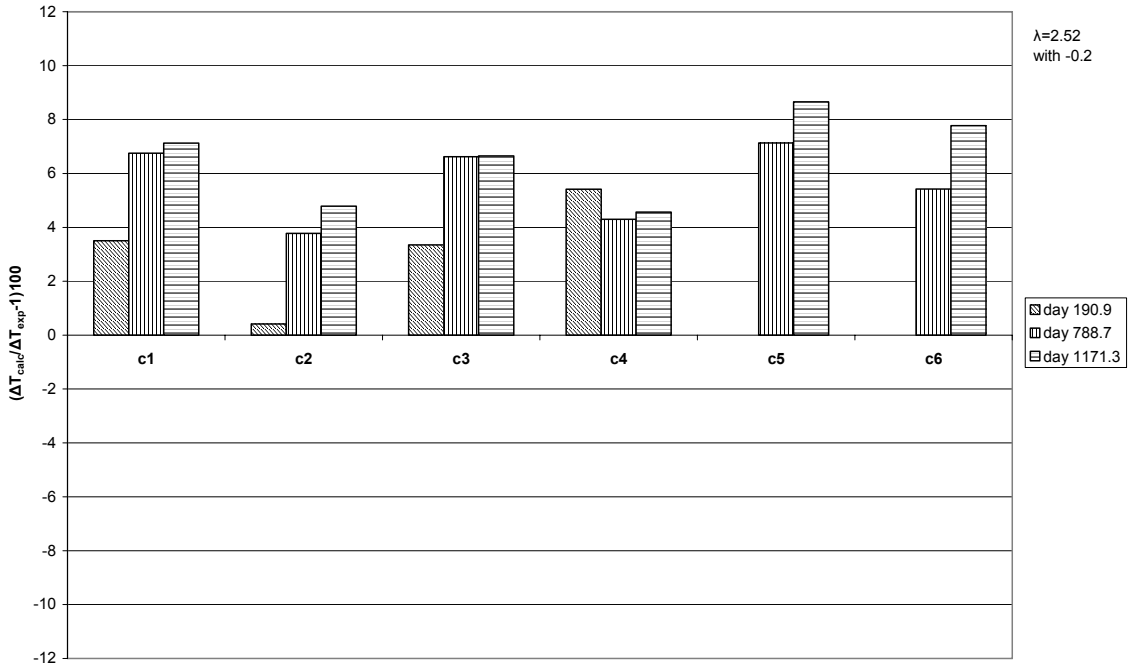

Figure 7-10. *λ = 2.52 W/(m·K), background temperature reduction.*

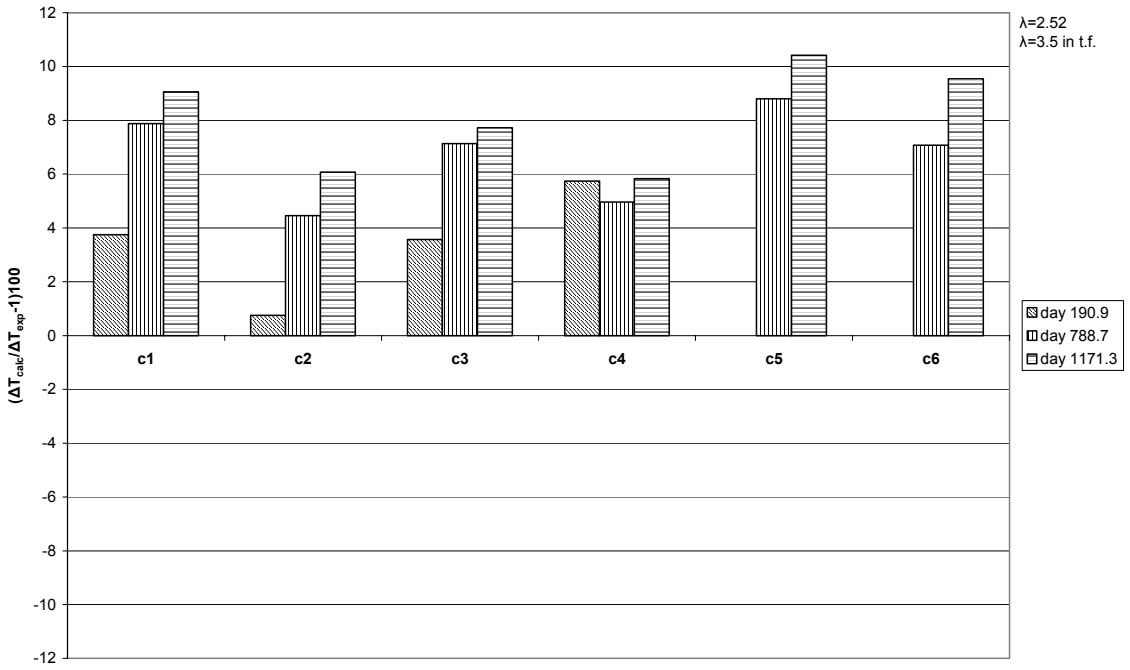

Figure 7-11. *λ = 2.52 W/(m·K), tunnel floor thermal conductivity 3.5 W/(m·K).*

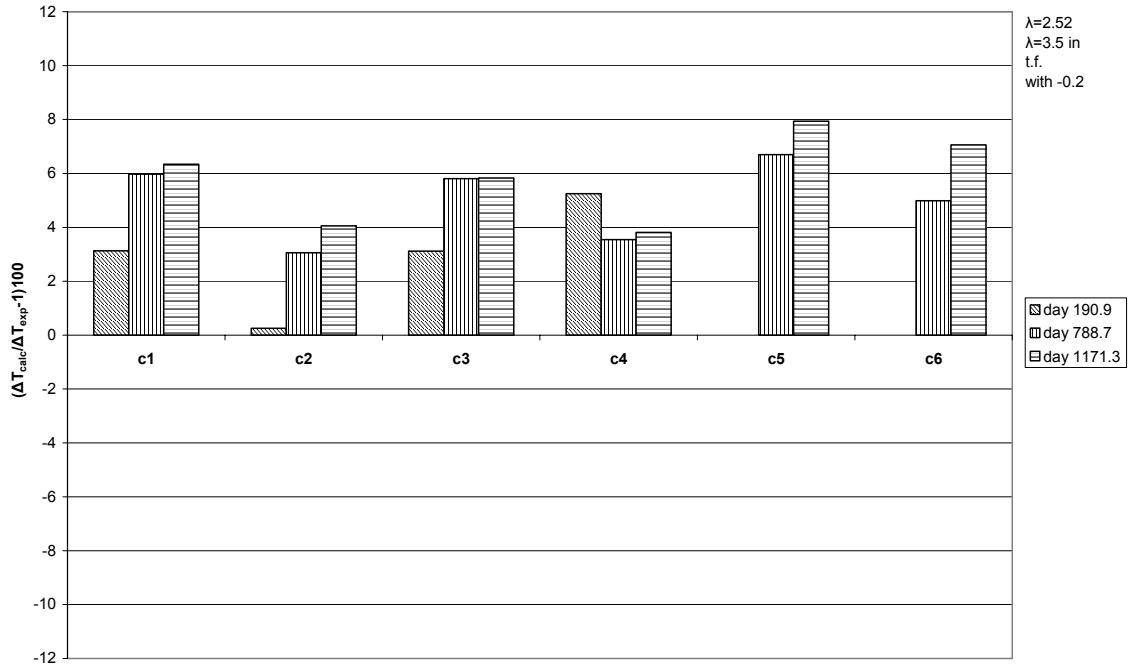

Figure 7-12. *λ = 2.52 W/(m·K), background temperature reduction, tunnel floor thermal conductivity 3.5 W/(m·K).*